A Fano Framework for Embeddings of Graphs in Surfaces

Blake Dunshee* M. N. Ellingham†

31 December 2024

Abstract

We consider seven fundamental properties of cellular embeddings of graphs in compact surfaces, and show that each property can be associated with a point of the Fano plane F, in such a way that allowable combinations of properties correspond to projective subspaces of F. This Fano framework allows us to deduce a number of implications involving the seven properties, providing new results and unifying existing ones. For each property, we provide a correspondence between embeddings with that property and an associated structure for 4-regular graphs, using the medial graph of the graph embedding. We apply this to characterize when a graph embedding has a twisted dual with one of the properties. For each allowable combination of properties, we show that a graph embedding with these properties exists. We investigate connections between the seven properties and three weaker 'Eulerian' properties. Our proofs involve parity conditions on closed walks in an extended version of the 'gem' (graph-encoded map) representation of a graph embedding.

1 Introduction

1.1 Summary of main results

Consider the following seven possible properties of a cellular embedding $\boldsymbol{G}$ of a finite graph in a compact surface:

(1) The underlying surface of $\boldsymbol{G}$ is orientable.

(2) A cycle in $\boldsymbol{G}$ is 1-sided if and only if it is odd.

(3) The underlying graph of $\boldsymbol{G}$ is bipartite.

(4) The embedding $\boldsymbol{G}$ is *directable*, meaning there exists an orientation (direction) of the edges of $\boldsymbol{G}$ so that every face boundary is a directed walk.

(5) The embedding $\boldsymbol{G}$ is 2-face-colorable.

(6) If $\boldsymbol{G}$ and its dual $\boldsymbol{G}^*$ are embedded together in their common underlying surface Σ in the natural way, then the resulting regions of $\Sigma - (\boldsymbol{G} \cup \boldsymbol{G}^*)$ can be properly 2-colored.

(7) The edges of $\boldsymbol{G}$ can be 2-colored so that the colors alternate around every vertex and around every face.

These properties seem somewhat arbitrary, although several of them involve some kind of 2-colorability or parity condition. In fact, the above properties are closely related and form a coherent framework. Each property can be described using bipartiteness of a particular graph derived from an embedded graph $\boldsymbol{G}$, or as a parity condition on cycles or closed walks in graphs known as the 'gem' and 'jewel' of $\boldsymbol{G}$. Using these

*Email: blake.dunshee@belmont.edu. College of Sciences and Mathematics, Belmont University, Nashville, TN 37212, U. S. A.

†Email: mark.ellingham@vanderbilt.edu. Department of Mathematics, Vanderbilt University, Nashville, TN 37240, U. S. A. Supported by Simons Foundation awards 429625 and MPS-TSM-00002760.

descriptions we can map these properties to points in the binary vector space $\mathbb{Z}_2^3$, where the zero vector corresponds to a trivial property satisfied by all graph embeddings, so that only the nonzero vectors are of interest. The nonzero vectors form a Fano plane, and the Fano plane structure gives connections between the properties.

Our main result can be stated in general terms as follows.

Fano Framework. *The seven properties above can be mapped to the points of the Fano plane F, so that for every embedded graph **G**, the properties satisfied by **G** form a projective subspace of F.*

In particular, the lines of the Fano plane can be described as follows. Given $a, b \in \{0, 1, 2, \ldots, 7\}$, compute $a \oplus b$ by turning a and b into 3-digit base 2 numbers, adding these as vectors in $\mathbb{Z}_2^3$, and then converting back to an integer. For example, $6 \oplus 3 = 110_2 \oplus 011_2 = 101_2 = 5$. This operation is commutative and associative, and is a special case of the well-known *Nim sum*. Now three properties (a), (b), and (c) with $a, b, c \in \{1, 2, \ldots, 7\}$ form a line in the Fano plane if and only if $a \oplus b \oplus c = 0$.

The Fano Framework has a number of consequences, such as the following metatheorem.

Metatheorem A. *Every embedded graph has exactly zero, one, three, or seven of the seven properties above. Thus, every combination of two properties implies a third property, and if four properties are satisfied then all seven properties hold.*

There are another two metatheorems which together give a specific theorem for any three of the seven properties.

Metatheorem B. *Let (a), (b), and (c) be distinct properties from the seven properties above, such that $a \oplus b \oplus c = 0$. Then any two of (a), (b), or (c) imply the third.*

Metatheorem C. *Let (a), (b), and (c) be distinct properties from the seven properties above, such that $a \oplus b \oplus c \neq 0$. Then the three properties (a), (b), and (c) together imply all seven properties.*

The rest of this section discusses important previous ideas that form the background for our work. Section 2 defines the machinery that we need for our proofs. Section 3 establishes the Fano Framework in terms of parity conditions for closed walks in gems or jewels, and Section 4 verifies that these conditions correspond to the seven properties above. Section 5 shows how bidirections of the medial checkerboard (a colored version of the medial graph) are related to the seven properties. These can be applied to give characterizations of when a twisted dual is orientable or bipartite. Section 6 investigates three weaker 'Eulerian' properties, which can also be characterized using parity conditions for a special type of closed walk, or using bidirections of the medial checkerboard. Section 7 provides examples of embeddings with all allowable combinations of the seven properties. While most of the results in this paper involve parity (i.e., modulo 2) conditions for closed walks in gems or jewels, Section 8 provides a result involving a congruence condition modulo 4 which characterizes embeddings all of whose partial duals are Eulerian, and also embeddings all of whose partial duals have a single vertex. Some concluding remarks appear in Section 9.

The major contributions of this paper are the overall framework, and the development of suitable tools to make the proofs easy. Our arguments are mostly elementary, but this is due to the careful choice and refinement of appropriate machinery. In addition to providing new results, our work unifies a number of results in the literature.

1.2 Historical background

Our work rests on three key ideas. The first is *dualities* for graph embeddings. The notion of *geometric duality* was originally considered for polyhedra, and then transferred to graph embeddings (maps). This concept may go back to antiquity, and was certainly known to Kepler in the early 17th century [24, p. 181] in connection with the Platonic solids. Another relevant concept is *Petrie duality*, which originated with ideas of skew polygons and zigzag walks [10, p. 202] in regular polyhedra, attributed by Coxeter to his collaborator J. F. Petrie. The interactions between geometric duality and Petrie duality were described independently by

Wilson [39] and Lins [26], giving an *action of the symmetric group S_3 on graph embeddings*, which includes a third duality operation, called 'opposite' by Wilson and 'phial' by Lins, and now usually known as *Wilson duality*.

The second key idea is representation of graph embeddings using 3-edge-colored cubic (3-regular) graphs. This was discovered independently by a number of researchers in the 1970s and early 1980s. Robertson [33] and Lins [26] represented embeddings of graphs in surfaces using 3-colored 3-regular graphs, which Lins called *graph-encoded maps* or *gems*. Bonnington and Little [3] showed how a number of aspects of topological graph theory can be developed in terms of gems. Others, such as Ferri [18] (building on earlier work by Pezzana [32] and Ferri and Gagliardi [19]) and Vince [36] used more general $(n+1)$-edge-colored $(n+1)$-regular graphs to represent decompositions of n-dimensional manifolds; Ferri called these *crystallizations*. References [20, 27] provide useful background, and [27] discusses connections with other combinatorial and algebraic descriptions of graph embeddings.

The contribution of Lins [26] is particularly important because it ties together the two key ideas above. Lins extended gems to 4-edge-colored 4-regular graphs (still representing an embedding of a graph in a surface), which we will call *jewels*, in which the S_3-action induced by geometric and Petrie dualities can be implemented simply by permuting three of the edge colors.

The third key idea is *partial dualities* for graph embeddings. Partial Petrie duality has been used for a long time. It was realized independently by a number of people in the late 1970s, including Alpert, Haggard (who attributed the idea to Edmonds around 1970), Ringel, and Stahl, that the rotation system representation of orientable embeddings could be extended to represent nonorientable embeddings by the use of what are now called *edge signatures*, taking values in $\{-1, 1\}$ (or sometimes $\{0, 1\}$). Partial Petrie duality just consists of 'twisting' some edges by flipping their signatures. This was used, for example, by Stahl [34], in one of the papers that introduced edge signatures, to show that the genera of nonorientable embeddings of a given graph form an interval. However, it is less obvious that there is also a partial version of geometric duality, and it was a major breakthrough when Chmutov [7] pointed this out in 2009. Chmutov's work was anticipated to some extent by work of Bouchet, who defined delta-matroids in [4], along with an operation $S \triangle N$ for a delta-matroid S and a subset N of its ground set. Bouchet showed in [5] that every graph embedding has an associated delta-matroid, but he did not investigate what changes in a graph embedding correspond to the $\triangle$ operation (which is often called 'twisting' or 'pivoting'); essentially these are partial geometric duals. Ellis-Monaghan and Moffatt [16, 17] combined partial geometric duality and partial Petrie duality, forming a *twisted duality* framework for graph embeddings, including an *action of S_3^E on embeddings of graphs with a given edge set E*, which refines the S_3-action of Wilson and Lins.

The simple way in which partial geometric duality can be implemented in gems was pointed out by one of the authors (Ellingham) and Zha [15], and by Chmutov and Vignes-Tourneret in the more general context of hypermaps [9]. Ellingham and Zha also observed that Lins' approach to implementing dualities by permuting edge colors in jewels can be extended to the whole twisted duality framework.

2 Graphs and Cellular Graph Embeddings

Here we summarize a number of definitions and known results (without proof). We define gems, jewels, and medial checkerboards, explain how they correspond to embedded graphs, and how twisted duality can be implemented in simple ways using gems and jewels.

We need to discuss structures with varying levels of detail, so we introduce some notational conventions. An abstract graph H is denoted using italics, an embedded graph $\boldsymbol{H}$ is denoted using bold italics (and its underlying graph is H), and a colored structure $\mathbf{H}$ (possibly including embedding information) is denoted using a bold upright font (with underlying graph H, and if appropriate, with associated embedded graph $\boldsymbol{H}$). If we mention an embedding property or substructure for a colored structure $\mathbf{H}$ we mean that property or substructure of the embedded graph $\boldsymbol{H}$. And if we mention a graph property or substructure of $\mathbf{H}$ or $\boldsymbol{H}$ we mean that property or substructure of the abstract graph H.

2.1 Graphs

In this paper all graphs are finite and may contain loops and multiple edges. Graphs may be disconnected or empty. We use standard graph theory terminology following [1] or [37]. As we allow loops and multiple edges, it will sometimes be convenient to consider an edge to consist of two *half-edges*, each incident with a vertex.

A graph G is *Eulerian* if it has a circuit (closed trail) containing all the edges and vertices of G. It is well known that a graph is Eulerian if and only if it is connected and every vertex has even degree. More generally, G is *even-vertex* if every vertex has even degree, whether or not G is connected.

A *direction* (or *orientation*) of a graph assigns a direction to each edge. (Later we also consider bidirections, which allow the halves of an edge to be directed independently.)

2.2 Embedded graphs and duality

We assume the reader has a general familiarity with embeddings of graphs in surfaces. All surfaces in this paper are compact (except that we sometimes discuss embeddings in the plane, which we think of as a topological subspace of a sphere). Surfaces may be disconnected. A graph embedding is *cellular* if every face is homeomorphic to an open 2-cell, i.e., an open disk. All embeddings in this paper are cellular unless otherwise indicated. In a cellular embedding $\boldsymbol{G}$, each isolated vertex of G is embedded in its own sphere, with one face, which we call an *isolated vertex component* of $\boldsymbol{G}$. The set of faces of $\boldsymbol{G}$ is denoted by $F(\boldsymbol{G})$. Cellular embeddings of graphs can be represented in various ways, including by rotation systems with edge signatures, or as ribbon graphs (also known as fatgraphs or reduced band decompositions). We refer the reader to [17, 21, 30] for details.

A fundamental property of graph embeddings is orientability. A surface is *orientable* if a consistent clockwise direction can be assigned everywhere on each connected component of the surface. A simple closed curve in a surface is either 1-*sided*, having a neighborhood homeomorphic to a Möbius strip, or 2-*sided*, having a neighborhood homeomorphic to a cylinder. A surface is orientable if and only if every simple closed curve in the surface is 2-sided. A graph embedding $\boldsymbol{G}$ is *orientable* if its underlying surface is orientable, which for cellular embeddings is equivalent to every cycle of G being embedded as a 2-sided curve. In the rotation system/edge signature representation of a graph embedding $\boldsymbol{G}$, a cycle is 1-sided if and only if it has an odd number of edges of signature -1 (this does not depend on the particular rotation system/edge signature representation).

An embedded graph $\boldsymbol{G}$ is *directable* if there is a direction of G such that each face of $\boldsymbol{G}$ is bounded by a directed closed walk.

We recall the definition of the *geometric dual* $\boldsymbol{G}^*$ (usually just called the *dual*) of an embedded graph $\boldsymbol{G}$ in a surface Σ. Insert a new vertex v_f in each face f of $\boldsymbol{G}$, and add one edge e^* crossing each edge e of $\boldsymbol{G}$, joining the vertices v_f and v_g corresponding to the (possibly equal) faces f and g on either side of e. The dual $\boldsymbol{G}^*$ consists of the vertices v_f and the edges e^* in the surface Σ. Each isolated vertex component of $\boldsymbol{G}$ corresponds to an isolated vertex component of $\boldsymbol{G}^*$. The dual embedding $\boldsymbol{G}^*$ is orientable if and only if the primal (original) embedding $\boldsymbol{G}$ is orientable.

We can also take the dual of some colored structures $\mathbf{H}$. Suppose $\mathbf{H}$ is a colored structure consisting of an embedded graph $\boldsymbol{H}$ with colors assigned to vertices, edges, or faces (possibly all three). Then to find $\mathbf{H}^*$ we dualize $\boldsymbol{H}$ and transfer edge colors to corresponding dual edges, and vertex colors to corresponding dual faces and vice versa. This will apply to barycentric subdivisions and gems (defined below), and subgraphs of these. We sometimes call $\mathbf{H}^*$ a *colored dual* to emphasize that colors are transferred.

We can also form the *Petrie dual* of a cellularly embedded graph $\boldsymbol{G}$ by twisting every edge of $\boldsymbol{G}$ (flipping the signature of every edge in a rotation scheme/edge signature representation); it is denoted by $\boldsymbol{G}^\times$. Alternatively, we can define $\boldsymbol{G}^\times$ in terms of the *zigzags* or *Petrie walks* of $\boldsymbol{G}$, closed walks that alternately turn right and left at each vertex (relative to a local orientation of the traverser of the walk) as we trace them around $\boldsymbol{G}$ until they close up. We start with the graph G, take a closed disk D_Z for each zigzag Z of $\boldsymbol{G}$, and identify the boundary of D_Z with Z, forming a surface in which G is embedded as $\boldsymbol{G}^\times$. The zigzags of $\boldsymbol{G}$ are the faces of

$\boldsymbol{G}^\times$, and conversely, the faces of $\boldsymbol{G}$ are the zigzags of $\boldsymbol{G}^\times$. Each isolated vertex component of $\boldsymbol{G}$ corresponds to an isolated vertex component of $\boldsymbol{G}^\times$. The underlying graph of $\boldsymbol{G}^\times$ is the same as the underlying graph of $\boldsymbol{G}$.

The *degree* of a face or zigzag of $\boldsymbol{G}$ is the length of the associated closed walk in G. We say $\boldsymbol{G}$ is *even-face* or *even-zigzag* if every face or zigzag, respectively, has even degree.

2.3 Gems, jewels, and medial checkerboards

The main representations we will use for a graph embedding $\boldsymbol{G}$ are gems, jewels, and medial checkerboards. Our treatment of gems and jewels loosely follows [3, 15, 26]. However, we modify some notation and terminology, and to link gems, jewels, and medial checkerboards to embedded graphs we also use barycentric subdivisions, which is an approach based on [3, 18, 19, 32, 36].

Isolated vertex components cause some minor difficulties in representing an embedded graph using a gem, jewel, medial checkerboard, or barycentric subdivision. For much of this subsection and the next subsection we will therefore focus on embedded graphs without isolated vertex components.

A *graph-encoded map* or *gem* $\mathbf{J}$ consists of a finite cubic graph J with a proper 3-edge-coloring $\gamma : E(J) \to \{\mathsf{v}, \mathsf{f}, \mathsf{a}\}$, such that the components of the 2-factor induced by edges of colors v and f are 4-cycles. The colors $\mathsf{v}, \mathsf{f}, \mathsf{a}$ are constants, and in figures we will follow the convention of [3] and indicate them by red, blue, and yellow, respectively. We think of $\mathsf{v}, \mathsf{f}, \mathsf{a}$ as vertex, facial, and auxiliary colors that describe the correspondence between $\mathbf{J}$ and an embedded graph $\boldsymbol{G}$.

A *bigon* in $\mathbf{J}$ is a cycle whose edges are colored alternately with two of the three colors. The bigons have three types:

(a) *e-squares*, whose edges are colored with v and f;

(b) *v-gons*, whose edges are colored with v and a; and

(c) *f-gons*, whose edges are colored with f and a.

These three sets of bigons will correspond naturally to the edges, vertices, and faces, respectively, of a cellularly embedded graph.

Every gem $\mathbf{J}$ has an associated embedded graph $\boldsymbol{J}$ which is obtained by taking a closed disk D_C for each bigon C in J and identifying the boundary of D_C with C, forming a surface in which J is embedded. Faces associated with e-squares, v-gons, and f-gons are called *e-faces*, *v-faces* and *f-faces*, respectively. So, although gems are purely combinatorial objects, we can regard them as embedded graphs when convenient.

To give the correspondence between embedded graphs and gems, we first define the *barycentric subdivision* $\mathbf{B}$ of an embedded graph $\boldsymbol{G}$ without isolated vertex components. Subdivide each edge e of $\boldsymbol{G}$ with a new vertex v_e, and color all edges of the resulting embedded graph $\boldsymbol{G}'$ with v. Now add a new vertex v_f inside each face f of $\boldsymbol{G}'$. Join v_f to each vertex of $\boldsymbol{G}$ on the boundary of f with an edge of color a, and to each vertex v_e on the boundary of f with an edge of color f. The resulting embedded graph with colored edges is $\mathbf{B}$, which is embedded in the same surfaces as $\boldsymbol{G}$. In Figure 1 we show a planar embedded graph $\boldsymbol{G}$, and in Figure 2 we show its barycentric subdivision.

We can identify the origin of each vertex of $\mathbf{B}$ with incident edges, calling it *type* V, F, *or* E, depending on whether its incident edges have colors in $\{\mathsf{v}, \mathsf{a}\}$, $\{\mathsf{f}, \mathsf{a}\}$, or $\{\mathsf{v}, \mathsf{f}\}$, respectively. The faces of $\mathbf{B}$ are the *flags* of $\boldsymbol{G}$, and each flag is bounded by a triangle whose edges use all three colors. We can recognize $\boldsymbol{G}$ inside $\mathbf{B}$, formed by vertices of type V joined by edges of color v subdivided by vertices of type E. We can also recognize $\boldsymbol{G}^*$, formed by vertices of type F joined by edges of color f subdivided by vertices of type E. The barycentric subdivision is an embedded graph $\boldsymbol{B}$ with added edge colors, and the embedding is important. The combinatorial information (graph B and edge coloring) can be the same for different embeddings of the same graph G, so is not sufficient to determine $\boldsymbol{G}$.

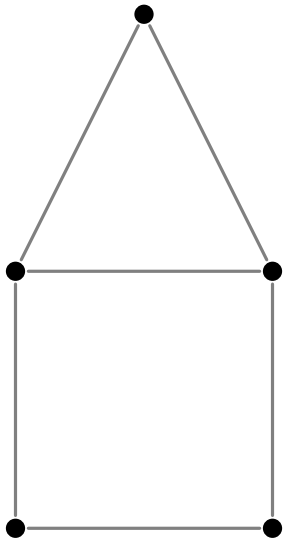

Figure 1: Embedded graph $\boldsymbol{G}$ for which we will take the barycentric subdivision and gem.

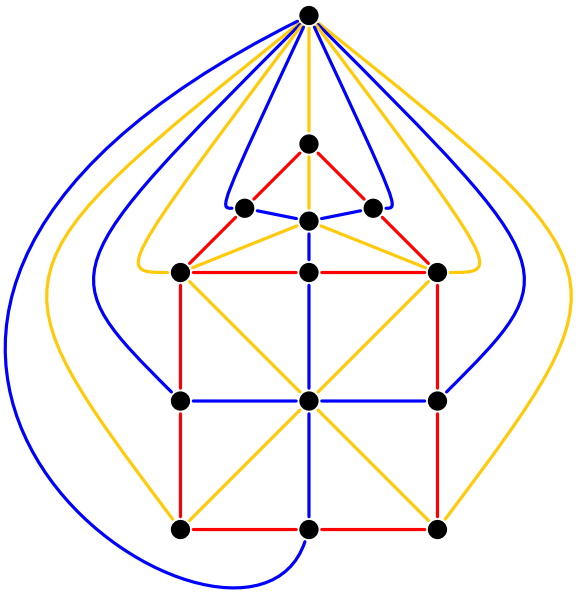

Figure 2: Barycentric subdivision of $\boldsymbol{G}$.

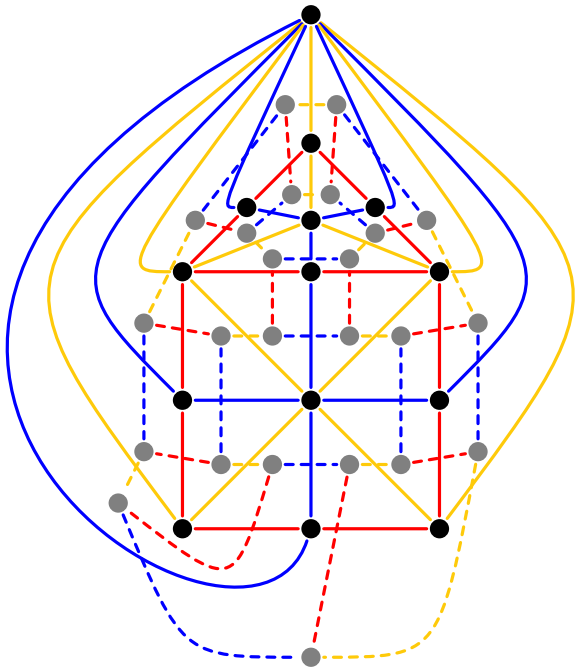

Figure 3: The barycentric subdivision (solid) and gem (dashed) for $\boldsymbol{G}$.

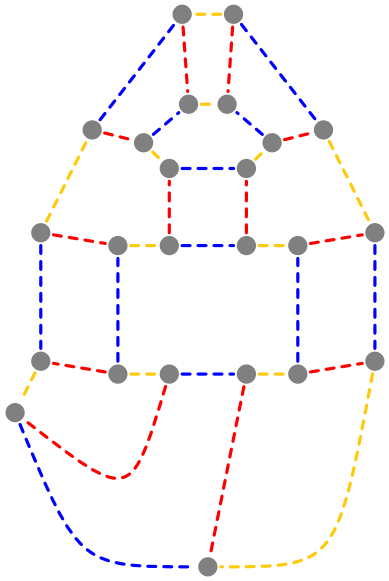

Figure 4: The gem of $\boldsymbol{G}$.

Now we can show that every embedded graph without isolated vertex components has a corresponding gem $\mathbf{J}$, and vice versa. The gem $\mathbf{J}$ of $\boldsymbol{G}$ is the colored dual $\mathbf{B}^*$ of $\mathbf{B}$. Like $\mathbf{B}$, this is embedded in the same surface as $\boldsymbol{G}$. Thus, each vertex of $\mathbf{J}$ represents a flag of $\boldsymbol{G}$ (so that $\mathbf{J}$ is sometimes called the *flag graph* of $\boldsymbol{G}$), and is incident with three edges of different colors. The v-gons, f-gons, and e-squares of $\mathbf{J}$ correspond to the vertices, faces, and edges, respectively, of $\boldsymbol{G}$. Conversely, if we have a gem $\mathbf{J}$, we can take its colored dual to obtain $\mathbf{B}$ and then recover $\boldsymbol{G}$ from $\mathbf{B}$. In Figure 3 we illustrate $\mathbf{B}$ and $\mathbf{J}$ together for the embedding of Figure 1, and in Figure 4 we show just $\mathbf{J}$.

A *jewel* is a slightly extended form of a gem, where we add edges of a new color z, associated with the zigzags of $\boldsymbol{G}$. Again following the conventions of [3], we use the color green for z in figures.

A jewel $\mathbf{L}$ consists of a 4-regular graph L with a proper 4-edge-coloring $\gamma : E(L) \to \{\mathsf{v}, \mathsf{f}, \mathsf{z}, \mathsf{a}\}$, such that each component of the 3-factor induced by edges of colors v, f and z is a complete graph K_4, which we call an *e-simplex*, and which contains an e-square consisting of its edges colored v and f. Jewels have v-gons and f-gons, defined in the same way as for gems, but also additional bigons whose edges are alternately colored a and z, which we call *z-gons*, and which correspond to the zigzags of $\boldsymbol{G}$. Unlike gems, a jewel $\mathbf{L}$ does not provide an embedding of its underlying graph L (so $\boldsymbol{L}$ is not defined).

Each jewel $\mathbf{L}$ has a corresponding gem $\mathbf{J}$ obtained by deleting the edges of color z, while we can obtain $\mathbf{L}$ from $\mathbf{J}$ by adding an edge of color z joining each pair of vertices that are diagonally opposite in an e-square of $\mathbf{J}$. It follows that there is also a correspondence between embedded graphs $\boldsymbol{G}$ without isolated vertex components and jewels $\mathbf{L}$.

If we have an edge-colored structure $\mathbf{H}$ (barycentric subdivision, gem, jewel) with edge-coloring γ, then for a color $c \in \{\mathsf{v}, \mathsf{f}, \mathsf{z}, \mathsf{a}\}$ we use $E^c_{\mathbf{H}}$ to denote $\gamma^{-1}(c)$, the set of edges colored c in $\mathbf{H}$. We will write $E^{\mathsf{v}}_{\mathbf{H}} \cup E^{\mathsf{f}}_{\mathbf{H}}$ as $E^{\mathsf{vf}}_{\mathbf{H}}$ and make other similar notational abbreviations.

A *medial checkerboard* $\mathbf{M}$ is a 4-regular graph embedding $\boldsymbol{M}$ with a proper 2-face-coloring $\gamma : F(\boldsymbol{M}) \to \{\mathsf{v}, \mathsf{f}\}$. Every embedded graph $\boldsymbol{G}$ without isolated vertex components has an associated medial checkerboard $\mathbf{M}$, and vice versa. Given an embedded graph $\boldsymbol{G}$, form the barycentric subdivision $\mathbf{B}$, and let $\boldsymbol{B'}$ be the embedded subgraph induced by all edges colored a.

The vertices of $\boldsymbol{B'}$ are the vertices of $\mathbf{B}$ of types V and F, and each face of $\boldsymbol{B'}$ has degree 4 and its interior contains a unique vertex of $\mathbf{B}$ of type E. Let $\boldsymbol{M}$ be the dual of $\boldsymbol{B'}$, using the vertices of type E in $\mathbf{B}$ as its vertices. Color each face of $\boldsymbol{M}$ with v or f depending on whether it contains a vertex of $\mathbf{B}$ of type V or F, respectively. The result is a medial checkerboard $\mathbf{M}$. Note that $\boldsymbol{B'}$, and hence $\mathbf{M}$, is embedded in the same surface as $\boldsymbol{G}$. We can also think of $\mathbf{M}$ as obtained from $\mathbf{B}$ by adding colors v and f to vertices of types V and F respectively, removing all vertices of type E (and their incident edges of colors v and f), uncoloring edges of color a, and then taking the colored dual.

Conversely, given a medial checkerboard $\mathbf{M}$, we can take the dual of $\boldsymbol{M}$ and use the color information from $\mathbf{M}$ to add back the remaining vertices, edges and colors of $\mathbf{B}$; from $\mathbf{B}$ we can recover $\boldsymbol{G}$.

In the literature the term "medial graph" may refer to the face-colored embedding $\mathbf{M}$, the embedding $\boldsymbol{M}$, or just the graph M. To remove this ambiguity, we use *medial graph* for M, *medial embedding* for $\boldsymbol{M}$, and *medial checkerboard* for $\mathbf{M}$. Also, the standard convention is to use the color black for faces of $\mathbf{M}$ corresponding to vertices of $\boldsymbol{G}$, and white for those corresponding to faces of $\boldsymbol{G}$ (see for example [16, 17]). However, we use v (red) and f (blue) for consistency with the colors in gems and jewels.

Note that $\mathbf{M}$ may also be obtained from the gem $\mathbf{J}$ by coloring the v- and f-faces with v and f, respectively, and contracting each e-face to a single vertex.

At this point we have developed correspondences between embedded graphs $\boldsymbol{G}$ without isolated vertex components, gems $\mathbf{J}$, jewels $\mathbf{L}$, and medial checkerboards $\mathbf{M}$ (and also barycentric subdivisions $\mathbf{B}$). For a given finite set E, the following are in one-to-one correspondence for a given finite set E: embedded graphs $\boldsymbol{G}$ with edge set E and no isolated vertex components (up to vertex relabeling and surface homeomorphism), gems $\mathbf{J}$ with e-squares labeled by E (up to color- and label-preserving isomorphism), jewels $\mathbf{L}$ with e-simplices labeled by E (up to color- and label-preserving isomorphism), and medial checkerboards $\mathbf{M}$ with vertices labeled by E (up to color- and label-preserving isomorphism and surface homeomorphism).

Finally, we address isolated vertex components. If $\boldsymbol{G}$ has isolated vertex components, we will just ignore them and use the other components of $\boldsymbol{G}$ to form the corresponding barycentric subdivision $\mathbf{B}$, gem $\mathbf{J}$, jewel

$\mathbf{L}$, or medial checkerboard $\mathbf{M}$. This means that we lose some information, and cannot uniquely reconstruct $\boldsymbol{G}$ from these other structures. We also lose the property that $\mathbf{B}$, $\mathbf{J}$, $\mathbf{L}$, and $\mathbf{M}$ are embedded in the same surface as $\boldsymbol{G}$. There are ways we could encode isolated vertex components in $\mathbf{B}$, $\mathbf{J}$, $\mathbf{L}$, or $\mathbf{M}$: for example, in [17] medial checkerboards $\mathbf{M}$ can contain gadgets called 'free loops' representing isolated vertex components. However, as we verify later in appropriate places, the presence or absence of isolated vertex components does not affect the properties we consider in this paper, so it is simpler to just disregard such components.

2.4 Twisted duality

Here we discuss duality operations, as investigated by Wilson [39] and Lins [26], and their extensions to twisted duality as defined by Ellis-Monaghan and Moffatt [16, 17], in terms of gems and jewels. We again follow [3, 15, 26].

In our work we will be applying operations such as duality or partial duality, which may completely rearrange vertices and faces, but essentially preserve the edge set of an embedded graph. For example, when we take the dual $\boldsymbol{G}^*$, the primal edge e of $\boldsymbol{G}$ and the dual edge e^* of $\boldsymbol{G}^*$ are different topological curves, but combinatorially we may consider them to be the same edge e, with different incidences in $\boldsymbol{G}$ and in $\boldsymbol{G}^*$, so that the underlying graphs of $\boldsymbol{G}$ and $\boldsymbol{G}^*$ have the same edge sets.

The dual $\boldsymbol{G}^*$ of a cellularly embedded graph $\boldsymbol{G}$ without isolated vertex components can easily be described in terms of gems. First we move from $\boldsymbol{G}$ to its associated gem $\mathbf{J}$. As observed by Lins [26], the gem $\mathbf{J}^{[*]}$ corresponding to $\boldsymbol{G}^*$ is formed by swapping the colors v and f everywhere in $\mathbf{J}$. This interchanges the v-gons and f-gons in the gem which cause vertices and faces to swap in the corresponding cellularly embedded graph. The dual also corresponds to swapping v and f in the jewel $\mathbf{L}$ to give a new jewel $\mathbf{L}^{[*]}$.

Note that $\mathbf{J}^{[*]}$ is different from $\mathbf{J}^*$ (which is $\mathbf{B}$), and $\mathbf{L}^{[*]}$ exists while $\mathbf{L}^*$ does not ($\mathbf{L}$ has no associated embedded graph). So our notation needs to distinguish between applying an operator such as duality directly to a colored structure $\mathbf{H}$, or applying it to $\boldsymbol{G}$ and making a corresponding change to $\mathbf{H}$. In general, when we apply an operation, such as duality, to an embedded graph $\boldsymbol{G}$, the corresponding operation on the associated colored structures $\mathbf{B}, \mathbf{J}, \mathbf{L}, \mathbf{M}$ will be denoted by enclosing the operation in brackets $[\cdot]$.

We can also define partial duality using gems (or jewels) [9, 15]. Suppose $\boldsymbol{G}$ is an embedded graph without isolated vertex components, and with corresponding gem $\mathbf{J}$ (or jewel $\mathbf{L}$). The *partial dual* $\boldsymbol{G} * A$ of $\boldsymbol{G}$ with respect to $A \subseteq E(G)$ can be obtained by swapping the colors v and f on the e-squares of $\mathbf{J}$ (or the e-simplices of $\mathbf{L}$) corresponding to A, to give the gem $\mathbf{J}[*A]$ (or jewel $\mathbf{L}[*A]$) that corresponds to $\boldsymbol{G}*A$. This is equivalent to the original definition of partial duality given by Chmutov [7], using arrow-marked ribbon graphs. Partial duals $\boldsymbol{G} * A$ generally have different underlying graphs, but they all have the same edge set, $E(G)$. Note that $\boldsymbol{G}^* = \boldsymbol{G} * E(G)$.

The Petrie dual of an embedded graph $\boldsymbol{G}$ without isolated vertex components can also be interpreted very simply in terms of the corresponding jewel $\mathbf{L}$. The jewel $\mathbf{L}^{[\times]}$ corresponding to $\boldsymbol{G}^\times$ is obtained by swapping the colors f and z everywhere in $\mathbf{L}$, which exchanges the f-gons and z-gons in $\mathbf{L}$ and hence exchanges the faces and zigzags in $\boldsymbol{G}$. We can also interpret the Petrie dual in terms of the gem $\mathbf{J}$: remove all edges colored f and then add new edges colored f joining opposite corners of each e-square of $\mathbf{J}$ to obtain $\mathbf{J}^{[\times]}$. Note that the underlying graph of $\mathbf{J}^{[\times]}$ is not J.

We can also form the *partial Petrie dual* $\boldsymbol{G} \times A$ with respect to $A \subseteq E(G)$ by twisting (flipping the signatures of) only the edges in A. The jewel $\mathbf{L}[\times A]$ corresponding to $\boldsymbol{G} \times A$ is obtained by swapping colors f and z just in the e-simplices of $\mathbf{L}$ that correspond to A, and the corresponding gem $\mathbf{J}[\times A]$ is obtained by moving the edges of color f just in the e-squares of $\mathbf{J}$ that correspond to A. Partial Petrie duals $\boldsymbol{G} \times A$ all have the same underlying graph G and hence the same edge set $E(G)$. Note that $\boldsymbol{G}^\times = \boldsymbol{G} \times E(G)$.

For embedded graphs $\boldsymbol{G}$ with isolated vertex components, we can implement all of the above operations (duality, partial duality, Petrie duality, partial Petrie duality) by applying them to the other components of $\boldsymbol{G}$, leaving the isolated vertex components unchanged.

We can apply sequences of duals and Petrie duals, which we compose left to right, so that, for example, $\boldsymbol{G}^{*\times} = (\boldsymbol{G}^*)^\times$. Since the dual and Petrie dual just permute the three colors $\mathsf{v}, \mathsf{f}, \mathsf{z}$ in a jewel $\mathbf{L}$, they generate the S_3-action discovered by Wilson [39] and Lins [26], with the relation that $\mathbf{L}^{[*\times*]} = \mathbf{L}^{[\times*\times]}$, so that

$\boldsymbol{G}^{*\times *} = \boldsymbol{G}^{\times *\times}$ for embedded graphs $\boldsymbol{G}$. Thus, there are at most six distinct embedded graphs that can be obtained from $\boldsymbol{G}$ in this way: $\boldsymbol{G}$, $\boldsymbol{G}^*$, $\boldsymbol{G}^\times$, $\boldsymbol{G}^{*\times}$, $\boldsymbol{G}^{\times *}$ and $\boldsymbol{G}^{*\times *} = \boldsymbol{G}^{\times *\times}$.

We can also compose partial duals and partial Petrie duals, to produce, for example, $\boldsymbol{G} * A \times B * C = ((\boldsymbol{G} * A) \times B) * C$ for $A, B, C \subseteq E(G)$. We use abbreviated notation when applying several operations to the same set of edges A, such as $\boldsymbol{G} \times *A$ to mean $G \times A * A$. Again the operations are composed left to right. A composition of partial dual and partial Petrie dual operations is a *twisted dual operation*, and an embedded graph obtained by applying a twisted dual operation to $\boldsymbol{G}$ is a *twisted dual* of $\boldsymbol{G}$. Ellis-Monaghan and Moffatt [16, 17] developed the idea of twisted duals and showed that twisted duals give an action of $S_3^{E(G)}$ on the embedded graphs derived from $\boldsymbol{G}$. This action can be interpreted as permuting the colors $\mathsf{v}, \mathsf{f}, \mathsf{z}$ independently in each e-simplex of the jewel $\mathbf{L}$, and extends the S_3-action generated by geometric and Petrie duality.

The *partial Wilson dual* of $\boldsymbol{G}$ with respect to A is defined as $\boldsymbol{G} \odot A = \boldsymbol{G} * \times * A$, which is also equal to $\boldsymbol{G} \times * \times A$. The partial Wilson dual corresponds to swapping colors v and z in the e-simplices corresponding to A in the jewel $\mathbf{L}$. The *Wilson dual* of $\boldsymbol{G}$ is $\boldsymbol{G}^\odot = \boldsymbol{G} \odot E(G) = \boldsymbol{G}^{*\times *} = \boldsymbol{G}^{\times *\times}$, which corresponds to swapping v and z everywhere in $\mathbf{L}$ to give $\mathbf{L}^{[\odot]}$.

Our notation here differs a little from what is generally used, but is more convenient for our purposes. The standard notation introduced by Chmutov [7] for the partial dual $\boldsymbol{G} * A$ is $\boldsymbol{G}^A$, but this becomes awkward when we need to take partial Petrie duals as well as partial duals. Ellis-Monaghan and Moffatt [16, 17] use δ to denote partial dual and τ to denote partial Petrie dual, so they would write $\boldsymbol{G}^{\delta(A)\tau(B)\delta(C)}$ for our $\boldsymbol{G} * A \times B * C$. Their operations $\delta(A)$ and $\tau(B)$ compose left to right, but δ and τ by themselves compose right to left, so that $\boldsymbol{G}^{\delta\tau(A)} = (\boldsymbol{G}^{\tau(A)})^{\delta(A)}$, which is our $\boldsymbol{G} \times *A = \boldsymbol{G} \times A * A$. In our notation twisted duality operations always compose left to right. Our notation is similar to that typically used for operations on delta-matroids.

3 Parity Conditions for Closed Walks in Gems and Jewels

3.1 Generalized bipartiteness

Our results are based on a generalization of the idea of bipartiteness in graphs. One condition equivalent to bipartiteness is that all closed walks have even length. We will extend this by choosing a set of edges, and investigating the condition that all closed walks contain an even number of edges from this set. We connect this with binary vertex labelings of G and with graphs obtained by contracting sets of edges in G.

A *v_0v_ℓ-walk* W in a graph G is a sequence of vertices and edges of G, $W = v_0e_1v_1e_2v_2 \ldots v_{\ell-1}e_\ell v_\ell$, where the incident vertices of each e_i are v_{i-1} and v_i; ℓ is the *length* of W. If $S \subseteq E(G)$, define $\nu_S(W)$ to be the number of i for which $e_i \in S$, i.e., the number of edges of W that belong to S, counted with their multiplicity in W.

We say W is *trivial* if $\ell = 0$, and *closed* if $v_0 = v_\ell$. We often use K to denote a closed walk. The following fundamental fact is well known.

Lemma 3.1. *In a graph G, a nontrivial closed walk $K = v_0e_1v_1e_2v_2...e_\ell(v_\ell = v_0)$ with no internal repeated vertex ($v_i \neq v_j$ for $0 \leq i < j < \ell$) is either a cycle or the walk $v_0e_1v_1e_1v_0$.*

By repeatedly breaking a closed walk into two shorter closed walks at an internal repeated vertex, and applying Lemma 3.1, we obtain the following.

Lemma 3.2. *Let G be a graph, let $S \subseteq E(G)$, and let K be a closed walk in G. If $\nu_S(K)$ is odd then there is a cycle C that is a (not necessarily consecutive) subsequence of K for which $\nu_S(C)$ is also odd.*

A *binary labeling* of a graph G is a function $\lambda : V(G) \to \mathbb{Z}_2$. If $S \subseteq E(G)$, then an *S-labeling* of G is a binary labeling such that for every edge e with ends u and v, $\lambda(u) \neq \lambda(v)$ if $e \in S$ and $\lambda(u) = \lambda(v)$ if $e \notin S$, or in other words, $\lambda(v) = (\lambda(u) + \nu_S(uev)) \bmod 2$. For $u \in V(G)$ we say λ is an *S-labeling relative to u* if $\lambda(u) = 0$. The following observations are easy but useful.

Observation 3.3. Let G be a graph and $u, w \in V(G)$.

(a) Every binary labeling λ of G is an S-labeling for a unique $S \subseteq E(G)$, namely $S = \{e \in E(G) \mid \lambda(u) \neq \lambda(w)$ where u and w are the endvertices of $e\}$.

(b) If λ is an S-labeling of G and W is a uw-walk in G, then $\lambda(w) = (\lambda(u) + \nu_S(W)) \bmod 2$.

(c) An S-labeling of G is unique up to flipping values (swapping 0 and 1) on components of G.

If $U \subseteq V(G)$ then S is the *coboundary of U in G* if S is the set of edges of G joining U to $V(G) - U$.

The graph $G \not\phi S$ is obtained from G by *contracting S in G*, by which we mean identifying vertices connected by edges of S, and then deleting the edges of S. Contracting S has the same result as contracting the edges in S individually, in any order. Contracting a loop is the same as deleting it. Every edge in $E(G) - S$ remains an edge of $G \not\phi S$, although non-loops of G may become loops of $G \not\phi S$. Contracting a set of edges S in a graph G does not correspond exactly to contracting S in an embedded graph $\boldsymbol{G}$ to form $\boldsymbol{G}/S$ (see the definition in [17, Section 4.2]), so we use different notation. However, if S does not induce any noncontractible cycles in $\boldsymbol{G}$, then the underlying graph of $\boldsymbol{G}/S$ is $G \not\phi S$.

We can now define a generalization of bipartiteness via several simple equivalent conditions, stated in Theorem 3.4. Conditions (a) and (b) are easily seen to be equivalent, (a) and (c) are equivalent by Lemma 3.2, and it is straightforward to prove that (a) $\Rightarrow$ (d) $\Rightarrow$ (e) $\Rightarrow$ (f) $\Rightarrow$ (a), so we omit the details.

Theorem 3.4. *Let G be a graph with $S \subseteq E(G)$. Then the following are equivalent:*

(a) *$\nu_S(K)$ is even for every closed walk K in G.*

(b) *For all $u, w \in V(G)$, $\nu_S(W)$ has the same parity for all uw-walks W in G.*

(c) *$\nu_S(C)$ is even for every cycle C in G.*

(d) *G has an S-labeling.*

(e) *S is a coboundary in G.*

(f) *$G \not\phi \overline{S}$ is bipartite, where $\overline{S} = E(G) - S$.*

If G and S satisfy any of the conditions in Theorem 3.4, we say that G is *S-bipartite*. Note that $E(G)$-bipartiteness is just bipartiteness, and we refer to an $E(G)$-labeling, with the two vertex classes of the bipartition labeled 0 and 1, as a *bipartite labeling* of G.

3.2 Main idea of this paper

At this point we can summarize our fundamental approach. The main idea of this paper is to translate properties of embedded graphs into parity conditions for closed walks in gems or jewels, of the form of Theorem 3.4(a). These conditions can then be combined using addition. We use other S-bipartiteness conditions as appropriate. We apply Theorem 3.4 frequently, usually without explicit reference.

The sets of edges S that we will be concerned with are the edges of prescribed colors in a gem or jewel. We simplify the notation for the function for counting the number of edges colored v in a walk in a jewel $\mathbf{L}$, namely $\nu_{E^{\mathsf{v}}_{\mathbf{L}}}$, to $v_{\mathbf{L}}$. Similarly, functions $f_{\mathbf{L}}$, $z_{\mathbf{L}}$, and $a_{\mathbf{L}}$ count the number of edges colored f, z and a, respectively. We use the same notation for a gem $\mathbf{J}$, except that we do not have $z_{\mathbf{J}}$. We will write $v_{\mathbf{L}}(K) + f_{\mathbf{L}}(K)$ as $(v + f)_{\mathbf{L}}(K)$, and use other similar abbreviations.

3.3 Some known results

Before discussing our full Fano Framework, we illustrate our main idea by re-proving two known results. We begin with the following.

Proposition 3.5 (Wilson [39], Ellis-Monaghan and Moffatt [16, 17])**.** *Let $\boldsymbol{G}$ be an orientable graph embedding. Then $\boldsymbol{G}$ is bipartite if and only if $\boldsymbol{G}^{\times}$ is orientable.*

Wilson [39, Theorem 3] stated Theorem 3.5 without proof for regular maps (graph embeddings with certain symmetry properties). Ellis-Monaghan and Moffatt, [16, Proposition 4.30(2)] and [17, Proposition 3.27], gave an incorrect statement of Wilson's result (corrected in the errata for [17], available from Moffatt's website), but a correct proof that applies to all graph embeddings, not just regular maps.

Applying Proposition 3.5 with $\boldsymbol{G}^\times$ replacing $\boldsymbol{G}$ shows that if $\boldsymbol{G}^\times$ is orientable and $\boldsymbol{G}^\times$ is bipartite (equivalent to $\boldsymbol{G}$ being bipartite), then $\boldsymbol{G}$ is orientable. Combining this with Proposition 3.5 gives the following stronger statement.

Theorem 3.6. *Let $\boldsymbol{G}$ be an embedded graph. Any two of the following properties imply the third:*

(a) *$\boldsymbol{G}$ is orientable.*

(b) *$\boldsymbol{G}$ is bipartite (or equivalently $\boldsymbol{G}^\times$ is bipartite).*

(c) *$\boldsymbol{G}^\times$ is orientable.*

Theorem 3.6 is in fact one case of Metatheorem B, since conditions (a), (b), and (c) are just properties (1), (2), and (3), respectively, of our original properties. (The equivalence between (c) and property (3) is discussed in Subsubsection 4.2.5.) We give a proof of the theorem using gems and generalized bipartiteness. Most of the work involves translating the properties of Theorem 3.6 into parity conditions for closed walks.

We rely on the following result to translate conditions (a) and (c) of Theorem 3.6.

Theorem 3.7 (Lins [26])**.** *Let $\boldsymbol{G}$ be a graph embedding with corresponding gem $\mathbf{J}$. Then $\boldsymbol{G}$ is orientable if and only if $\mathbf{J}$ is bipartite.*

If $\boldsymbol{G}$ has no isolated vertex components, Theorem 3.7 can be regarded as a consequence of a 1949 result of Tutte [35, p. 481], namely that a 3-face-colorable embedding of a cubic graph is orientable if and only if the graph is bipartite. This has been rediscovered a number of times. To apply it here, note that the partition of the faces of a gem into v-, f-, and e-faces provides a proper 3-face-coloring, and that $\mathbf{J}$ is orientable if and only if $\boldsymbol{G}$ is orientable, because they are embedded in the same surface. If $\boldsymbol{G}$ has isolated vertex components, they affect neither the orientability of $\boldsymbol{G}$ nor the bipartiteness of $\mathbf{J}$, so the result also holds in that case.

Since $(v + f + a)_{\mathbf{J}}$ counts all edges in a gem $\mathbf{J}$, Theorem 3.7 is equivalent to the following.

Corollary 3.8. *Let $\boldsymbol{G}$ be a graph embedding with corresponding gem $\mathbf{J}$. Then $\boldsymbol{G}$ (or equivalently $\boldsymbol{G}^*$) is orientable if and only if $(v + f + a)_{\mathbf{J}}(K)$ is even for all closed walks K in $\mathbf{J}$.*

We can also derive the following from Theorem 3.7.

Theorem 3.9. *Let $\boldsymbol{G}$ be a graph embedding with corresponding gem $\mathbf{J}$. Then $\boldsymbol{G}^\times$ (or equivalently $\boldsymbol{G}^{\times *}$) is orientable if and only if $(v + a)_{\mathbf{J}}(K)$ is even for all closed walks in $\mathbf{J}$.*

Proof. Suppose that $\boldsymbol{G}^\times$ is orientable. By Theorem 3.7, $\mathbf{J}^{[\times]}$ is bipartite and so has a bipartite labeling λ. The value of λ flips as we go along edges of color v or a in $\mathbf{J}$, as they are also edges of $\mathbf{J}^{[\times]}$. But the edges of color f in $\mathbf{J}$ join vertices that are distance 2 in $\mathbf{J}^{[\times]}$, and so the value of λ does not change on edges of color f in $\mathbf{J}$. Therefore, by Observation 3.3 we see that λ is an $E^{\mathsf{va}}_{\boldsymbol{J}}$-labeling of $\mathbf{J}$, and so $(v + a)_{\mathbf{J}}(K)$ is even for all closed walks K in $\mathbf{J}$.

Conversely, if $(v + a)_{\mathbf{J}}(K)$ is even for all closed walks in K, then there is an $E^{\mathsf{va}}_{\mathbf{J}}$-labeling λ in $\mathbf{J}$. By similar reasoning to the above, λ is a bipartite labeling of $\mathbf{J}^{[\times]}$, so $\mathbf{J}^{[\times]}$ is bipartite. Thus, $\boldsymbol{G}^\times$ is orientable by Theorem 3.7. □

The following addresses Theorem 3.7(b).

Theorem 3.10. *Let $\boldsymbol{G}$ be a graph embedding with corresponding gem $\mathbf{J}$. Then $\boldsymbol{G}$ (or equivalently $\boldsymbol{G}^\times$) is bipartite if and only if $f_{\mathbf{J}}(K)$ is even for all closed walks in $\mathbf{J}$.*

Proof. Suppose first that $\boldsymbol{G}$ has no isolated vertex components. From Theorem 3.4(a) and (f), $f_{\mathbf{J}}(K)$ is even for all closed walks K in $\mathbf{J}$ if and only if $H = J \not\phi E^{\mathsf{va}}_{\mathbf{J}}$ is bipartite. But H is just the result of contracting all v-gons in J, and is just G with each edge e replaced by two parallel edges (originally the two edges of color f in the e-square of $\mathbf{J}$ corresponding to e). Therefore, H is bipartite if and only if G is bipartite, i.e., $\boldsymbol{G}$ is bipartite.

If $\boldsymbol{G}$ has isolated vertex components, they can be discarded without affecting either $\mathbf{J}$ or the bipartiteness of $\boldsymbol{G}$, so the result also holds in that case. □

Notice that in the proofs above we used different parts of Theorem 3.4, involving parity conditions for closed walks, labelings, and contractions. Now that we have translated the conditions of Theorem 3.6 into parity conditions for closed walks, its proof is easy.

Proof of Theorem 3.6. Let $\mathbf{J}$ be the gem of $\boldsymbol{G}$. By Theorems 3.8, 3.9, and 3.10, the conditions of Theorem 3.6 become, respectively, the following.

(a) $(v + a + f)_{\mathbf{J}}(K)$ is even for all closed walks K in $\mathbf{J}$.

(b) $f_{\mathbf{J}}(K)$ is even for all closed walks K in $\mathbf{J}$.

(c) $(v + a)_{\mathbf{J}}(K)$ is even for all closed walks K in $\mathbf{J}$.

But given two of the functions $(v + a + f)_{\mathbf{J}}$, $f_{\mathbf{J}}$, and $(v + a)_{\mathbf{J}}$, the third can be obtained by either addition or subtraction, so any two of (a), (b), or (c) imply the third. □

The other known result that we re-prove here is the following. Recall that an embedding is *directable* if the edges can be directed so that every face boundary is a directed walk.

Theorem 3.11 (R.-X. Hao [22, Lemma 4.1])**.** *Let $\boldsymbol{G}$ be an orientable graph embedding. Then $\boldsymbol{G}$ is directable if and only if $\boldsymbol{G}$ is 2-face-colorable.*

Again, it turns out that this result can be strengthened, to the following.

Theorem 3.12. *Let $\boldsymbol{G}$ be an embedded graph. Any two of the following properties imply the third:*

(a) *$\boldsymbol{G}$ is orientable.*

(b) *$\boldsymbol{G}$ is 2-face-colorable.*

(c) *$\boldsymbol{G}$ is directable.*

This is also a special case of Metatheorem B, involving properties (1), (5), and (4). Condition (a) is equivalent to $\boldsymbol{G}^*$ being orientable, (b) is equivalent to $\boldsymbol{G}^*$ being bipartite, and (see Proposition 4.3 below) (c) is equivalent to $\boldsymbol{G}^{*\times}$ being orientable. Therefore, Theorem 3.12 is just Theorem 3.6 with $\boldsymbol{G}$ replaced by $\boldsymbol{G}^*$.

Alternatively, we could give an independent proof for Theorem 3.12 based on parity conditions for closed walks in the jewel $\mathbf{J}$ of $\boldsymbol{G}$. As we have shown (for (a)) or will show below (for (b) and (c)), conditions (a), (b), and (c) turn out to be equivalent to evenness of $(v + f + a)_{\mathbf{J}}(K)$, $v_{\mathbf{J}}(K)$, and $(f + a)_{\mathbf{J}}(K)$, respectively, for all closed walks K in $\mathbf{J}$. Thus, a proof similar to the proof of Theorem 3.6 above can be provided.

Not every theorem implied by Metatheorem B can be obtained just by applying Theorem 3.6 to one of the six embeddings $\boldsymbol{G}$, $\boldsymbol{G}^*$, $\boldsymbol{G}^\times$, $\boldsymbol{G}^{*\times}$, $\boldsymbol{G}^{\times *}$, or $\boldsymbol{G}^{*\times *}$. Metatheorem B implies seven theorems, and only three of them (Theorems 3.6 and 3.12, and one other) can be obtained in this way. The other four theorems are, as far as we know, new, and will be discussed in more detail later.

3.4 Gems versus jewels

In the previous subsection, our proofs related embedding properties to parity conditions for closed walks in gems. In fact, all seven of our properties for an embedded graph $\boldsymbol{G}$ can be described by a condition of the form

$$\mathrm{CW}(\mathbf{J}, \alpha_{\mathsf{v}}\alpha_{\mathsf{f}}\alpha_{\mathsf{a}}): \quad (\alpha_{\mathsf{v}}v + \alpha_{\mathsf{f}}f + \alpha_{\mathsf{a}}a)_{\mathbf{J}}(K) \text{ is even for all closed walks } K \text{ in } \mathbf{J},$$

where $\mathbf{J}$ is the gem of $\boldsymbol{G}$ and $\alpha_{\mathsf{v}}\alpha_{\mathsf{f}}\alpha_{\mathsf{a}}$ is a 01-string of length 3. This actually gives eight conditions, but if $\alpha_{\mathsf{v}} = \alpha_{\mathsf{f}} = \alpha_{\mathsf{a}} = 0$, we have a property trivially satisfied by all embeddings. Our theory can be developed using conditions for gems, as can be seen in an earlier version of this work in [14, Chapter 4]. However, a more symmetric approach, providing easier proofs of some results, uses conditions in the jewel $\mathbf{L}$ instead of the gem $\mathbf{J}$.

In the jewel $\mathbf{L}$ of $\boldsymbol{G}$ we naturally consider conditions of the form

$$\mathrm{CW}(\mathbf{L}, \alpha_{\mathsf{v}}\alpha_{\mathsf{f}}\alpha_{\mathsf{z}}\alpha_{\mathsf{a}}): \quad (\alpha_{\mathsf{v}}v + \alpha_{\mathsf{f}}f + \alpha_{\mathsf{z}}z + \alpha_{\mathsf{a}}a)_{\mathbf{L}}(K) \text{ is even for all closed walks } K \text{ in } \mathbf{L},$$

where $\alpha_{\mathsf{v}}\alpha_{\mathsf{f}}\alpha_{\mathsf{z}}\alpha_{\mathsf{a}}$ is a 01-string of length 4. But some choices of $\alpha_{\mathsf{v}}\alpha_{\mathsf{f}}\alpha_{\mathsf{z}}\alpha_{\mathsf{a}}$ give rise to conditions that are satisfied only in trivial ways. The remaining choices correspond to parity conditions for closed walks in gems, as we now show.

Theorem 3.13. *Suppose that* $\mathbf{L}$ *is a jewel and* $\mathbf{J}$ *is the corresponding gem. Let* $\alpha_{\mathsf{v}}, \alpha_{\mathsf{f}}, \alpha_{\mathsf{z}}, \alpha_{\mathsf{a}} \in \{0, 1\}$.

(a) *If* $\alpha_{\mathsf{v}} + \alpha_{\mathsf{f}} + \alpha_{\mathsf{z}}$ *is odd, then* $\mathrm{CW}(\mathbf{L}, \alpha_{\mathsf{v}}\alpha_{\mathsf{f}}\alpha_{\mathsf{z}}\alpha_{\mathsf{a}})$ *holds if and only if* $\mathbf{L}$ *is empty.*

(b) *If* $\alpha_{\mathsf{v}} + \alpha_{\mathsf{f}} + \alpha_{\mathsf{z}}$ *is even, then* $\mathrm{CW}(\mathbf{L}, \alpha_{\mathsf{v}}\alpha_{\mathsf{f}}\alpha_{\mathsf{z}}\alpha_{\mathsf{a}})$ *holds if and only if* $\mathrm{CW}(\mathbf{J}, \alpha_{\mathsf{v}}\alpha_{\mathsf{f}}\alpha_{\mathsf{a}})$ *holds.*

Proof. (a) Assume that $\alpha_{\mathsf{v}} + \alpha_{\mathsf{f}} + \alpha_{\mathsf{z}}$ is odd.

Suppose that $\mathrm{CW}(\mathbf{L}, \alpha_{\mathsf{v}}\alpha_{\mathsf{f}}\alpha_{\mathsf{z}}\alpha_{\mathsf{a}})$ holds. If $\mathbf{L}$ is nonempty then it has an e-simplex. Let K be any triangle in the e-simplex. Then K uses one edge of each color $\mathsf{v}, \mathsf{f}, \mathsf{z}$, and so $(\alpha_{\mathsf{v}}v+\alpha_{\mathsf{f}}f+\alpha_{\mathsf{z}}z+\alpha_{\mathsf{a}}a)_{\mathbf{L}}(K) = \alpha_{\mathsf{v}}+\alpha_{\mathsf{f}}+\alpha_{\mathsf{z}}$, which is odd, a contradiction. Therefore $\mathbf{L}$ is empty.

Conversely, if $\mathbf{L}$ is empty, $\mathrm{CW}(\mathbf{L}, \alpha_{\mathsf{v}}\alpha_{\mathsf{f}}\alpha_{\mathsf{z}}\alpha_{\mathsf{a}})$ is satisfied vacuously.

(b) Assume that $\alpha_{\mathsf{v}} + \alpha_{\mathsf{f}} + \alpha_{\mathsf{z}}$ is even.

Suppose that $\mathrm{CW}(\mathbf{L}, \alpha_{\mathsf{v}}\alpha_{\mathsf{f}}\alpha_{\mathsf{z}}\alpha_{\mathsf{a}})$ holds. Every closed walk K in $\mathbf{J}$ is also a closed walk in $\mathbf{L}$, and moreover $z(K) = 0$, so $(\alpha_{\mathsf{v}}v+\alpha_{\mathsf{f}}f+\alpha_{\mathsf{a}}a)_{\mathbf{J}}(K) = (\alpha_{\mathsf{v}}v+\alpha_{\mathsf{f}}f+\alpha_{\mathsf{z}}z+\alpha_{\mathsf{a}}a)_{\mathbf{L}}(K)$, which is even. Hence $\mathrm{CW}(\mathbf{J}, \alpha_{\mathsf{v}}\alpha_{\mathsf{f}}\alpha_{\mathsf{a}})$ holds.

Now suppose that $\mathrm{CW}(\mathbf{J}, \alpha_{\mathsf{v}}\alpha_{\mathsf{f}}\alpha_{\mathsf{a}})$ holds. There is $S \subseteq E(J)$ with $(\alpha_{\mathsf{v}}v + \alpha_{\mathsf{f}}f + \alpha_{\mathsf{a}}a)_{\mathbf{J}} = \nu_S$, and by Theorem 3.4, J has an S-labeling λ. Since $V(L) = V(J)$, by Observation 3.3, λ is an T-labeling of L for some $T \subseteq E(L)$, and furthermore $T = S \cup S'$ for some $S' \subseteq E(L) - E(J) = E^{\mathsf{z}}_{\mathbf{L}}$. We know that $\nu_T(K)$ is even for all closed walks K in $\mathbf{L}$ because the T-labeling λ of L exists. So to prove that $\mathrm{CW}(\mathbf{L}, \alpha_{\mathsf{v}}\alpha_{\mathsf{f}}\alpha_{\mathsf{z}}\alpha_{\mathsf{a}})$ holds it suffices to show that $\nu_T = (\alpha_{\mathsf{v}}v + \alpha_{\mathsf{f}}f + \alpha_{\mathsf{z}}z + \alpha_{\mathsf{a}}a)_{\mathbf{L}}$.

If $\alpha_{\mathsf{v}} = \alpha_{\mathsf{f}}$, then $\alpha_{\mathsf{z}} = 0$. Moreover, diagonally opposite pairs of vertices of a given e-square in J have equal λ values, and so the edges between such pairs in $\mathbf{L}$ do not belong to T. In other words, $E^{\mathsf{z}}_{\mathbf{L}} \cap T = \emptyset$ and so $T = S$. Therefore, in L we have $\nu_T = \nu_S = (\alpha_{\mathsf{v}}v + \alpha_{\mathsf{f}}f + \alpha_{\mathsf{z}}z + \alpha_{\mathsf{a}}a)_{\mathbf{L}}$ because $\alpha_{\mathsf{z}} = 0$.

If $\alpha_{\mathsf{v}} \neq \alpha_{\mathsf{f}}$, then $\alpha_{\mathsf{z}} = 1$. Moreover, diagonally opposite pairs of vertices of a given e-square in J have different λ values, and so the edges between such pairs in $\mathbf{L}$ belong to T. In other words, $E^{\mathsf{z}}_{\mathbf{L}} \subseteq T$ and so $T = S \cup E^{\mathsf{z}}_{\mathbf{L}}$. Therefore, in L we have $\nu_T = \nu_S + z_{\mathbf{L}} = (\alpha_{\mathsf{v}}v + \alpha_{\mathsf{f}}f + \alpha_{\mathsf{z}}z + \alpha_{\mathsf{a}}a)_{\mathbf{L}}$ because $\alpha_{\mathsf{z}} = 1$. □

In light of part (a), we will consider only conditions $\mathrm{CW}(\mathbf{L}, \alpha_{\mathsf{v}}\alpha_{\mathsf{f}}\alpha_{\mathsf{z}}\alpha_{\mathsf{a}})$ where $\alpha_{\mathsf{v}} + \alpha_{\mathsf{f}} + \alpha_{\mathsf{z}}$ is even. In that case, when moving from jewels to gems we just delete the term $\alpha_{\mathsf{z}}z$. When moving from gems to jewels we add a term $\alpha_{\mathsf{z}}z$ where α_{z} is an even parity check bit for α_{v} and α_{f} (i.e., α_{z} makes $\alpha_{\mathsf{v}} + \alpha_{\mathsf{f}} + \alpha_{\mathsf{z}}$ even).

Using Theorem 3.13 we can, for example, give a very easy proof of Theorem 3.9, as follows:

$\boldsymbol{G}^{\times}$ is orientable
⇔ (Theorem 3.8) $\mathrm{CW}(\mathbf{J}^{[\times]}, 111)$ holds: $(v + f + a)_{\mathbf{J}^{[\times]}}(K)$ is even for all closed walks K in $\mathbf{J}^{[\times]}$
⇔ (Theorem 3.13) $\mathrm{CW}(\mathbf{L}^{[\times]}, 1101)$ holds: $(v + f + a)_{\mathbf{L}^{[\times]}}(K)$ is even for all closed walks K in $\mathbf{L}^{[\times]}$

$\Leftrightarrow$ (Petrie dual swaps colors f and z in jewels) $\quad \mathrm{CW}(\mathbf{L}, 1011)$ holds: $(v+z+a)_{\mathbf{L}}(K)$ is even for all closed walks K in $\mathbf{L}$

$\Leftrightarrow$ (Theorem 3.13) $\quad \mathrm{CW}(\mathbf{J}, 101)$ holds: $(v+a)_{\mathbf{J}}(K)$ is even for all closed walks K in $\mathbf{J}$.

As this proof shows, a condition $\mathrm{CW}(\mathbf{L}, \alpha_{\mathsf{v}}\alpha_{\mathsf{f}}\alpha_{\mathsf{z}}\alpha_{\mathsf{a}})$ has an advantage over a condition $\mathrm{CW}(\mathbf{J}, \alpha_{\mathsf{v}}\alpha_{\mathsf{f}}\alpha_{\mathsf{a}})$ when taking some combination of duals and Petrie duals: we just modify $\mathrm{CW}(\mathbf{L}, \alpha_{\mathsf{v}}\alpha_{\mathsf{f}}\alpha_{\mathsf{z}}\alpha_{\mathsf{a}})$ using the corresponding permutation of the colors $\mathsf{v}, \mathsf{f}, \mathsf{z}$.

The following observation is trivial but we state it for later reference.

Observation 3.14. Suppose $\alpha, \alpha' \in \{0,1\}$. Let $\alpha \oplus \alpha' = (\alpha + \alpha') \bmod 2$ be the sum of α and α' considered as elements of $\mathbb{Z}_2$. Then $\alpha + \alpha'$, $\alpha - \alpha'$, and $\alpha \oplus \alpha'$ all have the same parity.

Suppose we know that two conditions $\mathrm{CW}(\mathbf{L}, \alpha)$ and $\mathrm{CW}(\mathbf{L}, \alpha')$ hold, where $\alpha = \alpha_{\mathsf{v}}\alpha_{\mathsf{f}}\alpha_{\mathsf{z}}\alpha_{\mathsf{a}}$ and $\alpha' = \alpha'_{\mathsf{v}}\alpha'_{\mathsf{f}}\alpha'_{\mathsf{z}}\alpha'_{\mathsf{a}}$, so that

$$(\alpha_{\mathsf{v}}v + \alpha_{\mathsf{f}}f + \alpha_{\mathsf{z}}z + \alpha_{\mathsf{a}}a)_{\mathbf{L}}(K) \text{ and } (\alpha'_{\mathsf{v}}v + \alpha'_{\mathsf{f}}f + \alpha'_{\mathsf{z}}z + \alpha'_{\mathsf{a}}a)_{\mathbf{L}}(K)$$

are even for all closed walks K in $\mathbf{L}$. Then clearly

$$((\alpha_{\mathsf{v}} + \alpha'_{\mathsf{v}})v + (\alpha_{\mathsf{f}} + \alpha'_{\mathsf{f}})f + (\alpha_{\mathsf{z}} + \alpha'_{\mathsf{z}})z + (\alpha_{\mathsf{a}} + \alpha'_{\mathsf{a}})a)_{\mathbf{L}}(K)$$

is even for all closed walks K in $\mathbf{L}$. But by Observation 3.14, this is equivalent to

$$((\alpha_{\mathsf{v}} \oplus \alpha'_{\mathsf{v}})v + (\alpha_{\mathsf{f}} \oplus \alpha'_{\mathsf{f}})f + (\alpha_{\mathsf{z}} \oplus \alpha'_{\mathsf{z}})z + (\alpha_{\mathsf{a}} \oplus \alpha'_{\mathsf{a}})a)_{\mathbf{L}}(K)$$

being even for closed walks K in $\mathbf{L}$. In other words, the condition $\mathrm{CW}(\mathbf{L}, \alpha \oplus \alpha')$ holds, where $\alpha \oplus \alpha'$ is the sum of α and α' considered as vectors in the vector space $\mathbb{Z}_2^4$. Similarly, if $\mathrm{CW}(\mathbf{J}, \widetilde{\alpha})$ and $\mathrm{CW}(\mathbf{J}, \widetilde{\alpha}')$ hold, where $\widetilde{\alpha}, \widetilde{\alpha}' \in \mathbb{Z}_2^3$, then $\mathrm{CW}(\mathbf{J}, \widetilde{\alpha} \oplus \widetilde{\alpha}')$ holds.

The conditions $\mathrm{CW}(\mathbf{L}, \alpha_{\mathsf{v}}\alpha_{\mathsf{f}}\alpha_{\mathsf{z}}\alpha_{\mathsf{a}})$ are of most interest when $\alpha_{\mathsf{v}} + \alpha_{\mathsf{f}} + \alpha_{\mathsf{z}}$ is even, i.e., when $\alpha_{\mathsf{v}} \oplus \alpha_{\mathsf{f}} \oplus \alpha_{\mathsf{z}} = 0$. The corresponding vectors $\alpha = \alpha_{\mathsf{v}}\alpha_{\mathsf{f}}\alpha_{\mathsf{z}}\alpha_{\mathsf{a}}$ form a 3-dimensional subspace Y of $\mathbb{Z}_2^4$. There is a basis for Y that is invariant under permutations of the first three coordinates, namely $\{0111, 1011, 1101\}$. These vectors correspond to the three functions

$$\overline{v}_{\mathbf{L}} = (f+z+a)_{\mathbf{L}}, \quad \overline{f}_{\mathbf{L}} = (v+z+a)_{\mathbf{L}}, \quad \text{and} \quad \overline{z}_{\mathbf{L}} = (v+f+a)_{\mathbf{L}},$$

which count all edges other than those of color v, f, or z, respectively. We therefore define another condition for a jewel $\mathbf{L}$ and $\beta = \beta_{\mathsf{v}}\beta_{\mathsf{f}}\beta_{\mathsf{z}} \in \mathbb{Z}_2^3$, namely

$\overline{\mathrm{CW}}(\mathbf{L}, \beta_{\mathsf{v}}\beta_{\mathsf{f}}\beta_{\mathsf{z}})$: $\quad (\beta_{\mathsf{v}}\overline{v} + \beta_{\mathsf{f}}\overline{f} + \beta_{\mathsf{z}}\overline{z})_{\mathbf{L}}(K)$ is even for all closed walks K in $\mathbf{L}$,

The conditions $\overline{\mathrm{CW}}(\mathbf{L}, \beta)$ have the same good behavior as conditions $\mathrm{CW}(\mathbf{L}, \alpha)$ under duals and Petrie duals: we can just modify the condition using the corresponding permutation of the colors $\mathsf{v}, \mathsf{f}, \mathsf{z}$. If $\overline{\mathrm{CW}}(\mathbf{L}, \beta)$ and $\overline{\mathrm{CW}}(\mathbf{L}, \beta')$ hold for $\beta, \beta' \in \mathbb{Z}_2^3$, then $\overline{\mathrm{CW}}(\mathbf{L}, \beta \oplus \beta')$ also holds, by similar reasoning to that used for conditions of the form $\mathrm{CW}(\mathbf{L}, \alpha)$. The correspondence between conditions $\mathrm{CW}(\mathbf{L}, \alpha)$ and $\overline{\mathrm{CW}}(\mathbf{L}, \beta)$ is easily determined, as follows.

Observation 3.15. Suppose $\mathbf{L}$ is a jewel, $\alpha = \alpha_{\mathsf{v}}\alpha_{\mathsf{f}}\alpha_{\mathsf{z}}\alpha_{\mathsf{a}} \in \mathbb{Z}_2^4$ with $\alpha_{\mathsf{v}} \oplus \alpha_{\mathsf{f}} \oplus \alpha_{\mathsf{z}} = 0$, and $\beta = \beta_{\mathsf{v}}\beta_{\mathsf{f}}\beta_{\mathsf{z}} \in \mathbb{Z}_2^3$. Then

(a) $\mathrm{CW}(\mathbf{L}, \alpha) \quad \Leftrightarrow \quad \overline{\mathrm{CW}}(\mathbf{L}, (\alpha_{\mathsf{v}} \oplus \alpha_{\mathsf{a}})(\alpha_{\mathsf{f}} \oplus \alpha_{\mathsf{a}})(\alpha_{\mathsf{z}} \oplus \alpha_{\mathsf{a}}))$, and

(b) $\overline{\mathrm{CW}}(\mathbf{L}, \beta) \quad \Leftrightarrow \quad \mathrm{CW}(\mathbf{L}, (\beta_{\mathsf{f}} \oplus \beta_{\mathsf{z}})(\beta_{\mathsf{v}} \oplus \beta_{\mathsf{z}})(\beta_{\mathsf{v}} \oplus \beta_{\mathsf{f}})(\beta_{\mathsf{v}} \oplus \beta_{\mathsf{f}} \oplus \beta_{\mathsf{z}}))$.

3.5 Proof of a Fano structure

We have now developed a vector space structure for embedded graph properties that can be represented as $\overline{\mathrm{CW}}(\mathbf{L}, \beta)$ (or, equivalently, as $\mathrm{CW}(\mathbf{L}, \alpha)$ or $\mathrm{CW}(\mathbf{J}, \widetilde{\alpha})$). This gives the overall Fano framework we wish to prove, subject to the following claim which describes the link between the properties of $\boldsymbol{G}$ from Section 1 and the properties $\overline{\mathrm{CW}}(\mathbf{L}, \beta)$. Define property (0) of a graph embedding $\boldsymbol{G}$ to be the always-true property. Let $b : \{0, 1, 2, \ldots, 7\} \to \mathbb{Z}_2^3$ be the bijection mapping each number to its representation as a 3-digit binary number, considered as a vector in $\mathbb{Z}_2^3$. For example, $b(3) = 011$.

Claim 3.16. Suppose $\boldsymbol{G}$ is an embedded graph with corresponding jewel $\mathbf{L}$. If $p \in \{0, 1, 2, \ldots, 7\}$ then property (p) for $\boldsymbol{G}$, from Section 1 or the previous paragraph, is equivalent to $\overline{\mathrm{CW}}(\mathbf{L}, b(p))$.

We postpone the proof, although at this point we could easily prove it for some values of p, such as $p = 1$.

Observation 3.17. If $p, p' \in \{0, 1, 2, \ldots, 7\}$ and $p \oplus p'$ is defined as in Section 1, then $b(p \oplus p') = b(p) \oplus b(p')$.

Now we can introduce the Fano plane. The *Fano plane* F has a standard representation as a Desarguesian projective plane over $\mathbb{Z}_2$: the *points* of F are the nonzero vectors of $\mathbb{Z}_2^3$, *d-dimensional projective subspaces* of F are $(d+1)$-dimensional vector subspaces of $\mathbb{Z}_2^3$ with 0 removed, and in particular a *line* of F consists of three nonzero vectors in $\mathbb{Z}_2^3$ whose sum is 0.

Theorem 3.18. *Let $\boldsymbol{G}$ be an embedded graph with corresponding jewel $\mathbf{L}$. Then $X = \{\beta \in \mathbb{Z}_2^3 \mid \overline{\mathrm{CW}}(\mathbf{L}, \beta)$ holds$\}$ is a vector subspace of $\mathbb{Z}_2^3$, and $X^- = X - \{0\}$ is a projective subspace of the Fano plane F.*

Proof. In a binary vector space a subset is a subspace if it contains 0 and is closed under addition. Since $\overline{\mathrm{CW}}(\mathbf{L}, 000)$ holds trivially for all $\mathbf{L}$, we have $0 = 000 \in X$. From discussion above after the definition of $\overline{\mathrm{CW}}(\mathbf{L}, \beta)$, we know that if $\beta, \beta' \in X$, then $\beta \oplus \beta' \in X$. Thus, X is a vector subspace of $\mathbb{Z}_2^3$ and hence X^- is a projective subspace of F. □

Proof of results in Section 1, subject to Claim 3.16. The Fano Framework as stated in Section 1 is obtained by translating the statement about X^- in Theorem 3.18 into a statement about properties of an embedded graph $\boldsymbol{G}$ using Claim 3.16. Metatheorem A follows because every d-dimensional projective subspace of F has $2^{d+1} - 1$ elements, where $d \in \{-1, 0, 1, 2\}$.

If $\overline{\mathrm{CW}}(\mathbf{L}, \cdot)$ holds for certain vectors of $\mathbb{Z}_2^3$, then by Theorem 3.18 it must also hold for all vectors in their span. If three nonzero vectors $\beta, \beta', \beta'' \in \mathbb{Z}_2^3$ satisfy $\beta \oplus \beta' \oplus \beta'' = 0$, then they are on a line in F, and each one is in the span of the other two. Thus, if $\overline{\mathrm{CW}}(\mathbf{L}, \cdot)$ holds for two of them, then it holds for the third. Translating this to properties of $\boldsymbol{G}$ using Claim 3.16 and Observation 3.17 yields Metatheorem B. If three nonzero vectors $\beta, \beta', \beta'' \in \mathbb{Z}_2^3$ satisfy $\beta \oplus \beta' \oplus \beta'' \neq 0$, then they are not on a line in F, and they span all of $\mathbb{Z}_2^3$, which translates to Metatheorem C. □

4 Graph embedding properties

In this section we consider the individual conditions $\overline{\mathrm{CW}}(\mathbf{L}, \beta)$ for $\beta \neq 0$, and establish their links to the graph embedding properties of Section 1, verifying Claim 3.16, and thus completing the proof of the Fano Framework. In some cases other equivalent properties are described as well. We also characterize the graphs G that possess an embedding satisfying each condition.

From now on we assume $\boldsymbol{G}$ is an embedded graph, $\mathbf{J}$ is its gem, and $\mathbf{L}$ is its jewel. We write '$\boldsymbol{G}$ satisfies condition (β)', for $\beta \in \mathbb{Z}_2^3$, to mean that $\mathbf{L}$ satisfies $\overline{\mathrm{CW}}(\mathbf{L}, \beta)$. All embedded graphs satisfy condition (000), and since $b(0) = 000$, Claim 3.16 holds for $p = 0$.

4.1 Orientability and bipartiteness of graph embeddings

Because we have carefully chosen our conditions (β) so that the effect of duals and Petrie duals is easy to track by permuting colors in $\mathbf{L}$, and hence permuting coordinates in β, we can see that three of our conditions (β) describe orientability of two embeddings, and three describe bipartiteness of two embeddings. To see which, we use Theorem 3.13 and Observation 3.15 to convert conditions for $\mathbf{J}$ into conditions (β) based on $\mathbf{L}$.

By Theorem 3.7, $\boldsymbol{G}$ (and $\boldsymbol{G}^*$) are orientable $\Leftrightarrow$ $(v + f + a)_{\mathbf{J}}$ is even for all closed walks K in $\mathbf{J}$ $\Leftrightarrow$ $(v + f + a)_{\mathbf{L}}(K) = \overline{z}(K)$ is even for all closed walks K in $\mathbf{L}$, i.e., (001) holds. Since the Petrie dual switches colors f and z in $\mathbf{L}$, we see that $\boldsymbol{G}^\times$ (and $\boldsymbol{G}^{\times *}$) are orientable if and only if (010) holds. Since the Wilson dual switches colors v and z in $\mathbf{L}$, we see that $\boldsymbol{G}^\odot = \boldsymbol{G}^{*\times *}$ (and $\boldsymbol{G}^{\odot *} = \boldsymbol{G}^{*\times}$) are orientable if and only if (100) holds. Thus, the three vectors of weight 1 in $\mathbb{Z}_2^3$ correspond to orientability properties.

Condition	Conditions, functions, and coboundary in $\mathbf{L}$	Condition, function, and coboundary in $\mathbf{J}$	Orientability/ bipartiteness
(001)	$\overline{\mathrm{CW}}(\mathbf{L}, 001) = \mathrm{CW}(\mathbf{L}, 1101)$ $\overline{z}_{\mathbf{L}} = (v + f + a)_{\mathbf{L}}$ $E_{\mathbf{L}}^{\mathsf{vfa}}$ is coboundary	$\mathrm{CW}(\mathbf{J}, 111)$ $(v + f + a)_{\mathbf{J}}$ $E_{\mathbf{J}}^{\mathsf{vfa}}$ is coboundary	$\boldsymbol{G}, \boldsymbol{G}^*$ orientable
(010)	$\overline{\mathrm{CW}}(\mathbf{L}, 010) = \mathrm{CW}(\mathbf{L}, 1011)$ $\overline{f}_{\mathbf{L}} = (v + z + a)_{\mathbf{L}}$ $E_{\mathbf{L}}^{\mathsf{vza}}$ is coboundary	$\mathrm{CW}(\mathbf{J}, 101)$ $(v + a)_{\mathbf{J}}$ $E_{\mathbf{J}}^{\mathsf{va}}$ is coboundary	$\boldsymbol{G}^\times, \boldsymbol{G}^{\times *}$ orientable
(011)	$\overline{\mathrm{CW}}(\mathbf{L}, 011) = \mathrm{CW}(\mathbf{L}, 0110)$ $(\overline{f} + \overline{z})_{\mathbf{L}}$ or $(f + z)_{\mathbf{L}}$ $E_{\mathbf{L}}^{\mathsf{fz}}$ is coboundary	$\mathrm{CW}(\mathbf{J}, 010)$ $f_{\mathbf{J}}$ $E_{\mathbf{J}}^{\mathsf{f}}$ is coboundary	$\boldsymbol{G}, \boldsymbol{G}^\times$ bipartite
(100)	$\overline{\mathrm{CW}}(\mathbf{L}, 100) = \mathrm{CW}(\mathbf{L}, 0111)$ $\overline{v}_{\mathbf{L}} = (f + z + a)_{\mathbf{L}}$ $E_{\mathbf{L}}^{\mathsf{fza}}$ is coboundary	$\mathrm{CW}(\mathbf{J}, 011)$ $(f + a)_{\mathbf{J}}$ $E_{\mathbf{J}}^{\mathsf{fa}}$ is coboundary	$\boldsymbol{G}^{*\times}, \boldsymbol{G}^{*\times *}$ orientable
(101)	$\overline{\mathrm{CW}}(\mathbf{L}, 101) = \mathrm{CW}(\mathbf{L}, 1010)$ $(\overline{v} + \overline{z})_{\mathbf{L}}$ or $(v + z)_{\mathbf{L}}$ $E_{\mathbf{L}}^{\mathsf{vz}}$ is coboundary	$\mathrm{CW}(\mathbf{J}, 100)$ $v_{\mathbf{J}}$ $E_{\mathbf{J}}^{\mathsf{v}}$ is coboundary	$\boldsymbol{G}^*, \boldsymbol{G}^{*\times}$ bipartite
(110)	$\overline{\mathrm{CW}}(\mathbf{L}, 110) = \mathrm{CW}(\mathbf{L}, 1100)$ $(\overline{v} + \overline{f})_{\mathbf{L}}$ or $(v + f)_{\mathbf{L}}$ $E_{\mathbf{L}}^{\mathsf{vf}}$ is coboundary	$\mathrm{CW}(\mathbf{J}, 110)$ $(v + f)_{\mathbf{J}}$ $E_{\mathbf{J}}^{\mathsf{vf}}$ is coboundary	$\boldsymbol{G}^{\times *}, \boldsymbol{G}^{*\times *}$ bipartite
(111)	$\overline{\mathrm{CW}}(\mathbf{L}, 111) = \mathrm{CW}(\mathbf{L}, 0001)$ $(\overline{v} + \overline{f} + \overline{z})_{\mathbf{L}}$ or $a_{\mathbf{L}}$ $E_{\mathbf{L}}^{\mathsf{a}}$ is coboundary	$\mathrm{CW}(\mathbf{J}, 001)$ $a_{\mathbf{J}}$ $E_{\mathbf{J}}^{\mathsf{a}}$ is coboundary	$\boldsymbol{M}$ bipartite

Table 1: Mapping between conditions and orientability/bipartiteness properties.

By Theorem 3.10, $\boldsymbol{G}$ (and $\boldsymbol{G}^\times$) are bipartite $\Leftrightarrow f_{\mathbf{J}}(K)$ is even for all closed walks K in $\mathbf{J} \Leftrightarrow (f+z)_{\mathbf{L}}(K)$ is even for all closed walks K in $\mathbf{L}$, i.e., $\mathrm{CW}(\mathbf{L}, 0110)$ holds $\Leftrightarrow (011)$ holds. Since duality switches colors v and f in $\mathbf{L}$, we see that $\boldsymbol{G}^*$ (and $\boldsymbol{G}^{*\times}$) are bipartite if and only if (101) holds. Since the Wilson dual switches colors v and z in $\mathbf{L}$, we see that $\boldsymbol{G}^\odot = \boldsymbol{G}^{\times *\times}$ (and $\boldsymbol{G}^{\odot\times} = \boldsymbol{G}^{\times *}$) are bipartite if and only if (110) holds. Thus, the three vectors of weight 2 in $\mathbb{Z}_2^3$ correspond to bipartiteness properties.

This leaves one condition, namely (111), which says that $(\overline{v}+\overline{f}+\overline{z})_{\mathbf{L}}(K) = a_{\mathbf{L}}(K)$ is even for all closed walks K in $\mathbf{L}$. By Theorem 3.4, this is equivalent to $L \not\phi E_{\mathbf{L}}^{\mathsf{vfz}}$ being bipartite, but that graph is exactly the medial graph M. So condition (111) is bipartiteness of M (or $\boldsymbol{M}$ or $\mathbf{M}$): the weight 3 vector in $\mathbb{Z}_2^3$ represents medial bipartiteness.

Table 1 summarizes these conclusions and shows the conditions in a number of forms, the corresponding edge-counting functions for closed walks in $\mathbf{L}$ and $\mathbf{J}$, and the corresponding binary labelings of $\mathbf{L}$ and $\mathbf{J}$. The conditions are in lexicographic order.

At this point the Fano structure shown in Figure 5 is apparent. The points represent the seven conditions. The lines (including the circle) represent the theorems coming from Metatheorem B: the points on each line are labeled by three vectors that sum to 0. The central point represents medial bipartiteness, and each of the six outer points represents either orientability or bipartiteness of two of the embedded graphs $\boldsymbol{G}, \boldsymbol{G}^*, \boldsymbol{G}^\times, \boldsymbol{G}^{*\times}, \boldsymbol{G}^{\times *}, \boldsymbol{G}^{*\times *}$. Each embedded graph is listed between the two points that represent its orientability and bipartiteness.

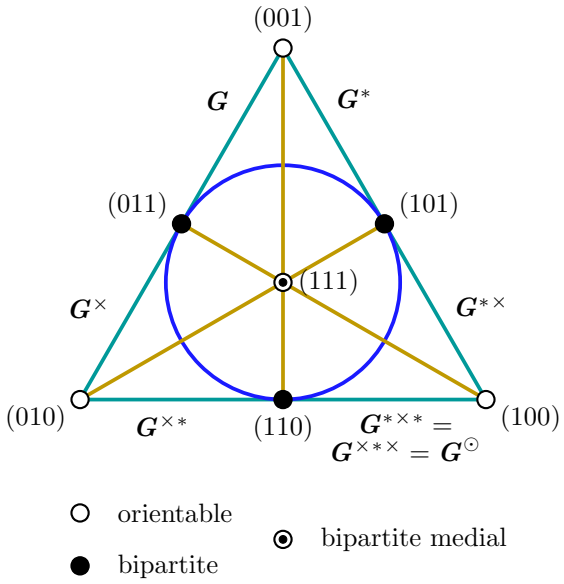

Figure 5: Fano Framework for Graph Embeddings.

The three sides of the triangle give theorems relating two orientability properties and one bipartiteness property: this includes Theorems 3.6 and 3.12, and a theorem derived by applying Theorem 3.6 to $\boldsymbol{G}^\odot = \boldsymbol{G}^{\times *\times}$ or $\boldsymbol{G}^{\odot\times} = \boldsymbol{G}^{\times *}$.

The three medians of the triangle give theorems relating one orientability property, medial bipartiteness and one bipartite property, and are to our knowledge new. One such result is Theorem 4.1 below; the other two can be obtained by applying this theorem to $\boldsymbol{G}^\times$ or $\boldsymbol{G}^{\times *}$, and to $\boldsymbol{G}^\odot = \boldsymbol{G}^{*\times *}$ or $\boldsymbol{G}^{\odot *} = \boldsymbol{G}^{*\times}$.

Theorem 4.1. *Let $\boldsymbol{G}$ be an embedded graph with medial checkerboard $\mathbf{M}$. Any two of the following properties imply the third:*

(a) *$\boldsymbol{G}$ (or $\boldsymbol{G}^*$) is orientable.*

(b) *$\mathbf{M}$ is bipartite.*

(c) *$\boldsymbol{G}^\odot = \boldsymbol{G}^{\times *\times}$ (or $\boldsymbol{G}^{\odot\times} = \boldsymbol{G}^{\times *}$) is bipartite.*

The circle gives one theorem relating three bipartiteness properties, which to our knowledge is also new.

Theorem 4.2. *Let $\boldsymbol{G}$ be an embedded graph. Any two of the following properties imply the third:*

(a) *$\boldsymbol{G}$ (or $\boldsymbol{G}^\times$) is bipartite.*

(b) *$\boldsymbol{G}^*$ (or $\boldsymbol{G}^{*\times}$) is bipartite.*

(c) *$\boldsymbol{G}^\odot = \boldsymbol{G}^{\times *\times}$ (or $\boldsymbol{G}^{\times *}$) is bipartite.*

4.2 Individual conditions and graph embedding properties

In this subsection we consider each condition (β) with $\beta \in \mathbb{Z}_2^3$, $\beta \neq 0$, for an embedded graph with gem $\mathbf{J}$ and jewel $\mathbf{L}$. We verify Claim 3.16 for $p = b^{-1}(\beta)$ by showing that (β) corresponds to the property (p) from Section 1, describe (β) in terms of bipartiteness of one or more graphs associated with $\boldsymbol{G}$, and in some cases discuss other properties equivalent to (β). (Each condition is also associated with a particular type of bidirection of the medial checkerboard $\mathbf{M}$, but we discuss this later, in Section 5.) We consider the values of β in increasing order by weight, and within each weight in an order that is convenient for our proofs.

4.2.1 Condition (001)

From Table 1, condition (001) means that $\boldsymbol{G}$ is orientable, which is property (1) from Section 1, as required.

By Theorem 3.7, condition (001) is equivalent to the gem $\mathbf{J}$ being bipartite.

There is also another graph whose bipartiteness is equivalent to condition (001). From Table 1, $(v + f + a)_{\mathbf{L}}(K)$ is even for all closed walks K in $\mathbf{L}$, which by Theorem 3.4 is equivalent to $L' = L \not\phi E^{\mathsf{z}}_{\mathbf{L}}$ being bipartite. The vertices of this graph correspond to the edges colored z in $\mathbf{L}$, the *diagonals* of the e-squares of $\mathbf{J}$. Each diagonal vertex is adjacent by four edges of colors v, f to the other diagonal of the same e-square, and by two edges of color z to two diagonals in adjacent e-squares. Replacing each group of four parallel edges of colors v, f in L' by a single edge gives a 3-regular graph called the *diagonal graph* of $\boldsymbol{G}$, whose bipartiteness is equivalent to condition (001).

Every graph G has an orientable embedding, i.e., an embedding satisfying condition (001).

4.2.2 Condition (010)

From Table 1, condition (010) means that $\boldsymbol{G}^{\times}$ is orientable. Thus, every cycle C of $\boldsymbol{G}^{\times}$ is 2-sided, i.e., if we take a rotation system/edge signature representation, each cycle has an even number of edges of signature -1. This is true if and only if, after we flip the signature of each edge to obtain a representation of $\boldsymbol{G}$, the even cycles of G have an even number of edges of signature -1, and the odd cycles have an odd number of edges of signature -1. In other words, a cycle in $\boldsymbol{G}$ is 1-sided if and only if it is odd. Thus, condition (010) is equivalent to property (2) of Section 1, as required.

The condition that $\boldsymbol{G}^{\times}$ be orientable has been used in the analysis of regular maps, beginning with Wilson [38], who called $\boldsymbol{G}$ 'pseudo-orientable' if this condition holds. More recently this property has been called 'bi-orientable' [8]. It can also be described by saying that each vertex can be given a rotation so that the rotations at the end of each edge are opposite. In other words, $\boldsymbol{G}$ has a representation using a rotation system and edge signatures in which every edge has signature -1.

By Theorem 3.7, condition (010) is equivalent to the gem of $\boldsymbol{G}^{\times}$, i.e., $\mathbf{J}^{[\times]}$, being bipartite.

There is also another graph whose bipartiteness is equivalent to condition (010). From Table 1, $(v + a)_{\mathbf{J}}(K)$ is even for all closed walks K in $\mathbf{J}$, which by Theorem 3.4 is equivalent to $J' = J \not\phi E^{\mathsf{f}}_{\mathbf{J}}$ being bipartite. The vertices of J' correspond to the edges colored f in $\mathbf{J}$, which represent the sides of the edges of $\boldsymbol{G}$. After reducing parallel edges in J' we obtain a 3-regular graph in which each side vertex is adjacent to the other side of the same edge and to the two sides consecutive with it around a face. This is called the *side graph* of $\boldsymbol{G}$, whose bipartiteness is equivalent to condition (010).

Since every graph G has an orientable embedding $\boldsymbol{G}$, it also has an embedding whose Petrie dual is orientable, namely $\boldsymbol{G}^{\times}$. So every graph has an embedding satisfying condition (010).

4.2.3 Condition (100)

From Table 1, condition (100) means that $\boldsymbol{G}^{*\times}$ is orientable. The following proposition shows that this is equivalent to property (4), which says that $\boldsymbol{G}$ is directable. This result is due to the authors and Joanna A. Ellis-Monaghan, and is equivalent to [31, Theorem 1] due to Nakamoto and Suzuki. We will give another proof in a future paper on directed embeddings; the proof in [31] is different from either of ours.

Proposition 4.3. *A graph embedding $\boldsymbol{G}$ is directable if and only if $\boldsymbol{G}^{*\times}$ is orientable.*

Proof. Suppose $\boldsymbol{G}$ is directable, and take a direction of its edges such that each face boundary is a directed walk. We can apply the direction of each edge of $\boldsymbol{G}$ to the corresponding edges of color f in $\mathbf{J}$. Then those edges in each f-gon point in the same direction around the f-gon, and those edges of each e-square point towards the same edge of color v. Each vertex of $\mathbf{J}$ can be labeled 0 or 1 according to whether its incident edge of color f is directed inwards or outwards, respectively. This is an $E^{\mathsf{fa}}_{\mathbf{J}}$-labeling of J, and so, by Theorem 3.4, $(f + a)_{\mathbf{J}}(K)$ is even for all closed walks K in $\mathbf{J}$, and hence, from Table 1, $\boldsymbol{G}^{*\times}$ is orientable.

This reasoning can be reversed, using an $E^{\mathsf{fa}}_{\mathbf{J}}$-labeling to define a suitable direction on edges of color f in $\mathbf{J}$ and hence on edges of $\boldsymbol{G}$. □

Condition (100) is also equivalent to $\boldsymbol{G}^{\odot}$ being orientable, which by Theorem 3.7 is equivalent to the gem of $\boldsymbol{G}^{\odot}$, which we denote as $\mathbf{J}^{[\odot]}$, being bipartite.

There is also another graph whose bipartiteness is equivalent to condition (100). From Table 1, $(f + a)_{\mathbf{J}}(K)$ is even for all closed walks K in $\mathbf{J}$, which by Theorem 3.4 is equivalent to $J'' = J \not\phi E^{\mathsf{v}}_{\mathbf{J}}$ being bipartite. The vertices of J'' correspond to the edges colored v in $\mathbf{J}$, which represent the ends of the edges (half-edges) of $\boldsymbol{G}$. After reducing parallel edges in J'' we obtain a 3-regular graph in which each end vertex is adjacent to the other end of the same edge and to the two ends consecutive with it around a vertex. This is called the *end graph* of $\boldsymbol{G}$, whose bipartiteness is equivalent to condition (100).

If $\boldsymbol{G}$ satisfies condition (100), then for each v-gon K in $\mathbf{J}$, $(f + a)_{\mathbf{J}}(K) = a_{\mathbf{J}}(K)$ is even, which means that the corresponding vertex has even degree. Thus, a connected graph with an embedding satisfying condition (100) must be Eulerian. This was pointed out by Lins [25, Theorem 2.9(b)].

To show the converse, that every Eulerian graph has an embedding satisfying condition (100), we use the following lemma. This is implicit in work of Bonnington, Conder, Morton and McKenna [2], and is closely related to Theorems 3.11 and 3.12.

Lemma 4.4. *Let D be an Eulerian digraph (having a closed directed trail that uses every arc exactly once). Then D has an orientable embedding in which the boundary of each face is a directed walk, and this embedding is 2-face-colorable.*

Corollary 4.5. *Every Eulerian graph G has an embedding that is orientable, 2-face-colorable, and directable.*

Proof. By following an Euler circuit T in G and orienting each edge of G in the direction of T, we obtain an Eulerian digraph D. Take an embedding $\boldsymbol{D}$ of D provided by Lemma 4.4, and discard the directions on the arcs to obtain an embedding $\boldsymbol{G}$ of G. This is clearly orientable, 2-face-colorable, and directable (add back directions to obtain $\boldsymbol{D}$). □

By Corollary 4.5, an Eulerian graph G has an embedding that is directable, i.e., it satisfies condition (100). Thus, a connected graph G has an embedding satisfying condition (100) if and only if it is Eulerian.

4.2.4 Condition (110)

From Table 1, condition (110) means that $\boldsymbol{G}^{\times *}$ (or $\boldsymbol{G}^{\times *\times}$) is bipartite. Since an embedded graph is bipartite if and only if its dual is 2-face-colorable, this is equivalent to $\boldsymbol{G}^{\times}$ (or $(\boldsymbol{G}^{\times *\times})^* = (\boldsymbol{G}^{*\times *})^* = \boldsymbol{G}^{*\times}$) being 2-face-colorable.

Since the faces of $\boldsymbol{G}^{\times}$ are the zigzags of $\boldsymbol{G}$ (and of $\boldsymbol{G}^*$), condition (110) is also equivalent to $\boldsymbol{G}$ being 2-zigzag-colorable, which means we can 2-color the zigzags so that the two zigzags sharing each edge are different colors (which implies that a zigzag cannot use the same edge twice).

We wish to show that condition (110) is equivalent to property (6) from Section 1, which says that if $\boldsymbol{G}$ and its dual $\boldsymbol{G}^*$ are embedded together in their common underlying surface Σ in the natural way, then the resulting regions of $\Sigma - (G \cup G^*)$ can be properly 2-colored. Embedding $\boldsymbol{G}$ and $\boldsymbol{G}^*$ simultaneously, adding a new vertex at the intersection of each edge and its dual edge, gives $\mathbf{B} \setminus E^{\mathsf{a}}_{\mathbf{B}}$, which we will call $\boldsymbol{G} \cup \boldsymbol{G}^*$. We must show that this is 2-face-colorable.

We may assume that $\boldsymbol{G}$ has no isolated vertex components. When we form $\mathbf{B}$ we ignore isolated vertex components of $\boldsymbol{G}$, so by the above definition $\boldsymbol{G} \cup \boldsymbol{G}^*$ also has no information regarding such components. While we could take the union of an isolated vertex component and its dual in a single sphere, this would consist of two vertices embedded in a sphere, which is problematic because it is not a cellular embedding.

A face of $\mathbf{B} \setminus E^{\mathsf{a}}_{\mathbf{B}}$ is called a *corner* of the embedded graph $\boldsymbol{G}$; it represents an incidence between a vertex and a face in $\boldsymbol{G}$. Each corner contains two flags with a common edge of color a. The corners of $\boldsymbol{G}$ therefore correspond to edges of color a in $\mathbf{B}$, edges of color a in $\mathbf{J}$, or edges of $\mathbf{M}$. The *corner graph* of $\boldsymbol{G}$ is the

underlying graph of $(\mathbf{B} \setminus E^{\mathsf{a}}_{\mathbf{B}})^*$, a 4-regular graph in which two vertices representing corners are joined by an edge when those corners are consecutive around a vertex or a face. From this it is apparent that the corner graph is also the medial graph of the medial embedding $\boldsymbol{M}$ of $\boldsymbol{G}$.

Using the duality between deletion and contraction, and noting that the edges in $\mathbf{J}$ of color a do not induce any cycles, we see that the corner graph is $J \oplus E^{\mathsf{a}}_{\mathbf{J}}$. But from Table 1, condition (110) means that $(v+f)_{\mathbf{J}}$ is even for all closed walks K in $\mathbf{J}$, and by Theorem 3.4 this is equivalent to the corner graph $J \oplus E^{\mathsf{a}}_{\mathbf{J}}$ being bipartite, which is equivalent to $\boldsymbol{G} \cup \boldsymbol{G}^* = \mathbf{B} \setminus E^{\mathsf{a}}_{\mathbf{B}}$ being 2-face-colorable, as required.

Condition (110) is also equivalent to the Petrie dual of the medial embedding, $\boldsymbol{M}^\times$, being orientable. To see this, observe that the medial embedding is always 2-face-colorable, so that $\boldsymbol{M}^*$ is always bipartite. Therefore, applying Figure 5 to $\boldsymbol{M}$, the medial graph of $\boldsymbol{M}$ (i.e., the corner graph of $\boldsymbol{G}$) being bipartite is equivalent to $\boldsymbol{M}^\times$ being orientable.

If a graph G has an embedding satisfying condition (110), then $\boldsymbol{G}^{\times *}$ is bipartite, which means that $\boldsymbol{G}^\times$ is 2-face-colorable, which implies that each vertex of its underlying graph, which is just G, has even degree. Thus, a connected graph with an embedding satisfying condition (110) must be Eulerian.

Conversely, if G is Eulerian then by Corollary 4.5 G has a 2-face-colorable embedding $\boldsymbol{G}$. Now $\boldsymbol{G}^\times$ is also an embedding of G, and $(\boldsymbol{G}^\times)^\times = \boldsymbol{G}$ is 2-face-colorable. In other words, $\boldsymbol{G}^\times$ is an embedding of G satisfying condition (110).

Thus, a connected graph has an embedding satisfying condition (110) if and only if it is Eulerian.

4.2.5 Condition (011)

From Table 1, condition (011) is equivalent to $\boldsymbol{G}$ (or $\boldsymbol{G}^\times$) being bipartite, which is property (3) from Section 1. Since an embedded graph is bipartite if and only if its dual is 2-face-colorable, this is equivalent to $\boldsymbol{G}^*$ (or $(\boldsymbol{G}^{\times *})$ being 2-face-colorable.

Condition (011) is also equivalent to condition (110) after swapping colors v and z in the jewel, i.e., after taking the Wilson dual. Therefore, it is equivalent to bipartiteness of the corner graph of $\boldsymbol{G}^\odot$, or the *Wilson corner graph*. This graph has the same vertex set as the corner graph of $\boldsymbol{G}$, but two vertices representing corners are joined by an edge when those corners are consecutive around a face or a zigzag of $\boldsymbol{G}$.

The class of graphs that have an embedding satisfying condition (011) is the set of all bipartite graphs; any embedding satisfies the condition.

4.2.6 Condition (101)

From Table 1, condition (101) is equivalent to $\boldsymbol{G}^*$ (or $\boldsymbol{G}^{*\times}$) being bipartite. Since an embedded graph is bipartite if and only if its dual is 2-face-colorable, this is equivalent to $\boldsymbol{G}$ (or $(\boldsymbol{G}^{*\times *})$ being 2-face-colorable, which is property (5) from Section 1.

Condition (101) is also equivalent to condition (110) after swapping colors f and z in the jewel, i.e., after taking the Petrie dual. Therefore, it is equivalent to bipartiteness of the corner graph of $\boldsymbol{G}^\times$, or the *Petrie corner graph*. This graph has the same vertex set as the corner graph of $\boldsymbol{G}$, but two vertices representing corners are joined by an edge when those corners are consecutive around a vertex or a zigzag of $\boldsymbol{G}$.

If a graph G has an embedding $\boldsymbol{G}$ satisfying condition (101), then $\boldsymbol{G}$ is 2-face-colorable, which obviously means that every vertex has even degree. Thus, if G is connected, G is Eulerian. Conversely, suppose that G is Eulerian. By Corollary 4.5, G has an embedding that is 2-face-colorable, i.e., it satisfies condition (101). Thus, a connected graph has an embedding satisfying condition (101) if and only if it is Eulerian.

4.2.7 Condition (111)

As indicated in Table 1, condition (111) is equivalent to bipartiteness of the medial checkerboard $\mathbf{M}$ of an embedded graph $\boldsymbol{G}$. A proper 2-coloring of the vertices of $\mathbf{M}$ translates to a coloring of the edges of $\boldsymbol{G}$ where colors alternate around each vertex and around each face, so condition (111) is equivalent to property (7) of Section 1.

If G has an embedding $\boldsymbol{G}$ satisfying property (7), with edges colored (say) black and white around each vertex and each face, then the degree of each vertex is even. Thus, if G is connected then it is Eulerian. Moreover, the numbers of half-edges colored black and white must be equal, so the numbers of edges colored black and white must be equal, and so $|E(G)|$ must be even.

Conversely, suppose G is an Eulerian graph and $|E(G)|$ is even. Let T be an Euler circuit in G. Because $|E(T)| = |E(G)|$ is even, we can color the edges of T alternately black and white, resulting in an equal number of black and white half-edges incident with each vertex. Choose a rotation scheme at each vertex that alternates black and white half-edges, and assign all edges signature 1. The result is an embedding $\boldsymbol{G}$ that satisfies property (7), and is moreover orientable.

Thus, a connected graph has an embedding satisfying condition (111), or equivalently property (7), if and only if it is Eulerian and has an even number of edges.

4.2.8 Summary

We have now verified Claim 3.16 by showing that that seven properties listed in the introduction (Section 1) correspond to the seven Fano conditions in Table 1. We will henceforth refer to these as the seven 'Fano properties'.

In Table 2 we give a full overview of the results in this section. The first column gives the appropriate condition and corresponding property from Section 1. The second column gives equivalent embedding properties. The third column gives associated graphs, not already mentioned in the second column, whose bipartiteness corresponds to the condition. The fourth column summarizes some results from Section 5 regarding bidirections of the medial checkerboard. The final column describes the connected graphs that have an embedding satisfying the given condition.

We have given a number of different ways to describe condition (110), which appear in the table. We can similarly describe conditions (011) and (101) in several ways, but we omit these for brevity.

We will provide examples to show that all combinations of the Fano properties allowed by Metatheorem A actually occur. However, we postpone this to Section 7, since it is helpful to first discuss three further 'Eulerian' properties and their connections with the Fano properties.

5 Medial checkerboard bidirections

In this section we link the seven Fano plane conditions for an embedded graph $\boldsymbol{G}$ to structures in the medial checkerboard $\mathbf{M}$. We use correspondences as follows:

Fano condition(s) for $\boldsymbol{G}$
$\leftrightarrow$ binary labeling(s) of gem $\mathbf{J}$ or jewel $\mathbf{L}$
$\leftrightarrow$ condition for edges colored a in $\mathbf{J}$ or $\mathbf{L}$
$\leftrightarrow$ structure in medial checkerboard $\mathbf{M}$.

The last step here relies on the fact that edges of $\mathbf{M}$ can be identified with edges of color a in $\mathbf{J}$ or $\mathbf{L}$, because we can think of M as either $J\phi(E(J) - E^{\mathsf{a}}_{\mathbf{J}})$ or $L\phi(E(L) - E^{\mathsf{a}}_{\mathbf{L}})$. A similar approach appears in the proof of Proposition 4.3 above: there we used correspondences between condition (100), an $E^{\mathsf{fa}}_{\mathbf{J}}$-labeling of the gem $\mathbf{J}$, and a condition for edges colored f in $\mathbf{J}$.

Our work extends and systematizes some previous results in the literature, which involve directions of the medial graph M. We work with *bidirections*, which assign a direction to each half-edge of a graph G. An edge is *directed* if its two halves are directed the same way, and *antidirected* if they are directed oppositely. We think of a *direction* as a bidirection where all edges are directed, and an *antidirection* is a bidirection where all edges are antidirected. An antidirected edge is *introverted* or *extraverted* depending on whether the halves are directed, respectively, into or out of the center of the edge, or equivalently, out of or into their incident vertices.

Medial graphs are 4-regular, and the bidirections that matter to us have special properties. In a 4-regular graph with a bidirection, a vertex is *balanced* if it has two incoming half-edges and two outgoing half-

Condition and property	Embedding properties (all equivalent)	(Other) associated bipartite graphs	Bidirection of $\mathbf{M}$	Connected graphs having embedding
(001) (1)	$\boldsymbol{G}, \boldsymbol{G}^*$ orientable	gem $\mathbf{J}$, diagonal graph	b-direction	all
(010) (2)	$\boldsymbol{G}^\times, \boldsymbol{G}^{\times *}$ orientable; cycle 1-sided $\Leftrightarrow$ odd; vertex rotations that reverse along edges	$\mathbf{J}^{[\times]}$, side graph	d-direction	all
(011) (3)	$\boldsymbol{G}, \boldsymbol{G}^\times$ bipartite; $\boldsymbol{G}^*, \boldsymbol{G}^{\times *}$ 2-face-colorable	Wilson corner graph	c-antidirection	bipartite
(100) (4)	$\boldsymbol{G}^{*\times}, \boldsymbol{G}^{*\times *}$ orientable; directable	$\mathbf{J}^{[\odot]}$, end graph	c-direction	Eulerian
(101) (5)	$\boldsymbol{G}^*, \boldsymbol{G}^{*\times}$ bipartite; $\boldsymbol{G}, \boldsymbol{G}^{*\times *}$ 2-face-colorable	Petrie corner graph	d-antidirection	Eulerian
(110) (6)	$\boldsymbol{G}^{\times *}, \boldsymbol{G}^{*\times *}$ bipartite; $\boldsymbol{G}^\times, \boldsymbol{G}^{*\times}$ 2-face-colorable; $\boldsymbol{G}, \boldsymbol{G}^*$ 2-zigzag-colorable; $\boldsymbol{G} \cup \boldsymbol{G}^*$ 2-face-colorable; $\boldsymbol{M}^\times, \boldsymbol{M}^{\times *}$ orientable	corner graph = medial graph of $\boldsymbol{M}$	b-antidirection	Eulerian
(111) (7)	$\mathbf{M}$ bipartite; can 2-color edges so alternate around vertices and faces		t-direction	Eulerian with even number of edges

Table 2: Summary of individual conditions.

edges, and *total* if all half-edges are incoming or all half-edges are outgoing. A bidirection is *balanced*, *total*, or *balanced-total* if every vertex is balanced, every vertex is total, or every vertex is balanced or total, respectively.

We will show that each individual Fano plane condition corresponds to a particular subclass of balanced-total directions or antidirections of M, with conditions involving the structure added to M to form the medial checkerboard $\mathbf{M}$ (i.e., vertex rotations and face colorings). In Section 6 we will expand this to include three additional properties. We also discuss how these bidirections interact with partial duality and partial Petrie duality. Allowable combinations of properties corresponding to lines in the Fano plane, or the whole Fano plane, can also be related to structures in the medial checkerboard: to do this we will use multiple binary labelings simultaneously,

5.1 Previous results on medial graph directions

The use of directions (orientations) of the medial graph to characterize embedding properties was introduced by Huggett and Moffatt [23]. Deng, Jin, and Metsidik extended this in various ways [13, 29, 28] to bidirections and additional properties. These results characterized when partial duals of an embedded graph $\boldsymbol{G}$ have certain properties. We describe some known results of this kind here; additional results are discussed in Subsection 6.2.

Definition 5.1. Suppose an embedded graph $\boldsymbol{G}$, with medial checkerboard $\mathbf{M}$, and a bidirection δ of the medial graph M, are given. A vertex v_e of $\mathbf{M}$, corresponding to $e \in E(G)$, is

(a) a *b-vertex* if the half-edge directions around v_e alternate (in (towards v_e), out (away from v_e), in, out);

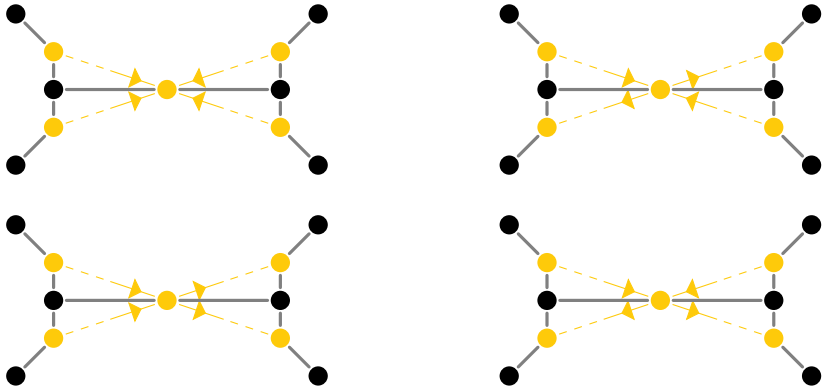

Figure 6: Top: t^-- and b-vertices; bottom: c- and d-vertices.

(b) a *c-vertex* if the half-edge directions and face colors around v_e are in the cyclic order (in, v, in, f, out, v, out, f);

(c) a *d-vertex* if the half-edge directions and face colors around v_e are in the cyclic order (in, f, in, v, out, f, out, v); and

(d) a *t-vertex* if the half-edge directions around v_e are (in, in, in, in) (a *t^--vertex*) or (out, out, out, out) (a *t^+-vertex*).

See Figure 6. Note that these definitions depend on both the bidirection δ and the vertex rotations and face colorings of $\mathbf{M}$. But we consider δ to be attached to the medial graph M, not the complete medial checkerboard $\mathbf{M}$, because we will consider the same δ for different medial checkerboards when we take twisted duals. If we have a balanced-total bidirection of M then these four types (with two subtypes of t-vertex) classify all vertices of $\mathbf{M}$.

An edge e in $\boldsymbol{G}$ is called a *b-edge*, *c-edge*, *d-edge*, or *t-edge* (or *t^--edge* or *t^+-edge*) according to the type of the corresponding vertex v_e in $\mathbf{M}$. We use *b-direction of* $\mathbf{M}$ (or *b-direction of* $\boldsymbol{G}$) to refer to a direction of M in which all vertices of $\mathbf{M}$ are b-vertices, *bc-antidirection of* $\mathbf{M}$ to refer to an antidirection of M in which all vertices of $\mathbf{M}$ are b- or c-vertices, and other similar terminology.

Note that if we reverse a balanced-total bidirection, or reverse it on some of the components of M, then it remains a balanced-total bidirection and the types of the vertices of $\mathbf{M}$ or edges of $\boldsymbol{G}$ remain unchanged.

Huggett and Moffatt [23] defined c- and d-edges. The idea of t-edges was used implicitly by Metsidik [28] and defined by Deng, Jin, and Metsidik [13], as part of results we will discuss in Section 6. The definition of b-edges is new and will be used later in this section. In the literature cd-bidirections are called *all-crossing* bidirections, and cdt-bidirections are called *crossing-total* bidirections. We now state some results from [13, 23].

Theorem 5.2 (Huggett and Moffatt [23, Theorem 1.3])**.** *Let $\boldsymbol{G}$ be a planar graph embedding with medial graph M and $A \subseteq E(G)$. Then the partial dual $\boldsymbol{G} * A$ is bipartite if and only if there exists a direction of M for which all elements of A are c-edges of $\boldsymbol{G}$ and all elements of $E(G) - A$ are d-edges of $\boldsymbol{G}$.*

Deng, Jin, and Metsidik [13] extended Theorem 5.2 to all embedded graphs, orientable or nonorientable, using directions of a 'modified medial graph', which depends on the choice of local rotations for the vertices of $\boldsymbol{G}$. Their result can also be expressed using bidirections of M with both directed and antidirected edges. We will not discuss the details, as there is a simpler way to handle the general case, which we describe in Subsection 5.5. In the orientable case, Deng, Jin, and Metsidik's modified medial graph is just the medial graph, and they obtain the following straightforward generalization of Theorem 5.2.

Theorem 5.3 (Deng, Jin, and Metsidik [13, Corollary 3.2])**.** *Let $\boldsymbol{G}$ be an orientable graph embedding with medial graph M and $A \subseteq E(G)$. Then $\boldsymbol{G} * A$ is bipartite if and only if there exists a direction of M for which all elements of A are c-edges of $\boldsymbol{G}$ and all elements of $E(G) - A$ are d-edges of $\boldsymbol{G}$.*

Taking $A = \emptyset$, Theorem 5.3 implies that an orientable embedded graph $\boldsymbol{G}$ is bipartite if and only there is a d-direction of its medial graph. But we know that an orientable $\boldsymbol{G}$ is bipartite if and only if $\boldsymbol{G}^\times$ (or $\boldsymbol{G}^{\times *}$) is orientable, i.e., $\boldsymbol{G}$ satisfies condition (010). This suggests that there is a d-direction of $\boldsymbol{G}$ if and only if condition (010) holds. One direction of this was verified by Yan and Jin.

Theorem 5.4 (Yan and Jin [40, Lemma 6.2])**.** *If a graph embedding $\boldsymbol{G}$ satisfies condition (010), i.e., $\boldsymbol{G}^\times$ is orientable, then there exists a d-direction of $\boldsymbol{G}$.*

We will unify and extend the above results in the next three subsections.

5.2 Medial checkerboard bidirections and jewels

In this subsection we establish a general connection between medial checkerboard bidirections and embedding properties using binary labelings of jewels. Theorems 5.2 and 5.3 involve properties of partial duals; we will show that characterization of the properties and the effect of taking twisted duals (partial duals, partial Petrie duals, and their compositions) can be considered independently.

The following observation is obvious, but stated for later reference.

Observation 5.5. Let $\boldsymbol{G}$ be an embedded graph with medial graph M, and let δ be a bidirection of M. Every edge $e \in E(G)$ is a b-, c-, or d-edge of $\boldsymbol{G}$ if and only if δ is a balanced bidirection, and every edge $e \in E(G)$ is a t-edge of $\boldsymbol{G}$ if and only if δ is a total bidirection.

The next observation is important for translating conditions between a medial checkerboard and a jewel.

Observation 5.6. Suppose $\boldsymbol{G}$ is an embedded graph with medial checkerboard $\mathbf{M}$ and jewel $\mathbf{L}$. Let $e \in E(G)$, let v_e be the vertex of $\mathbf{M}$ corresponding to e, and let $\mathbf{T}_e$ be the e-simplex of $\mathbf{L}$ corresponding to e.

(a) Each half-edge g of M incident with v_e corresponds to a half-edge g' of L colored a in $\mathbf{L}$, and incident with a vertex of $\mathbf{T}_e$.

(b) This gives a correspondence between bidirections δ of M and bidirections δ_L of the edges of L colored a in $\mathbf{L}$: a half-edge g of M is directed into or out of v_e by δ if and only if g' is directed into or out of $\mathbf{T}_e$ by δ_L, respectively.

(c) Half-edges g and h of $\mathbf{M}$ are consecutive in the rotation around v_e if and only if g' and h' are incident with consecutive vertices x and y of the e-square in $\mathbf{T}_e$. Moreover, the color of the face between g and h in $\mathbf{M}$ is the same as the color of the edge of $\mathbf{L}$ joining x and y.

Suppose that $\boldsymbol{G}$ is an embedded graph with medial checkerboard $\mathbf{M}$ and jewel $\mathbf{L}$. Using Observation 5.6(a) and (b), we set up a correspondence between a bidirection δ of M and a binary labeling λ of L by assigning 0 or 1 to each $x \in V(L)$ according to whether the unique bidirected half-edge incident with x is directed into or out of x by δ_L, respectively. We write $\lambda = \tau(\delta)$, and τ is a bijection, so $\delta = \tau^{-1}(\lambda)$.

Note that the correspondence between half-edges of M and certain half-edges of L is not affected by taking twisted duals. Thus, the correspondence between δ, δ_L, and $\lambda = \tau(\delta)$ is also not affected by taking twisted duals. The type of a vertex of the medial checkerboard $\mathbf{M}$ may change under taking a twisted dual, but the correspondence described in Observation 5.6(c) holds both for the original embedding and for the modified embedding.

Given δ and $\lambda = \tau(\delta)$, we know λ is an S-labeling for some unique $S \subseteq E(L)$. Then δ is a direction if and only if for each $e \in E^{\mathsf{a}}_{\mathbf{L}}$ with endpoints x and y, $\lambda(x) \neq \lambda(y)$, which is equivalent to $E^{\mathsf{a}}_{\mathbf{L}} \subseteq S$. Therefore, by Table 1 the conditions (001), (010), (100), and (111) correspond to medial checkerboard directions. Similarly, δ is an antidirection if and only if $S \cap E^{\mathsf{a}}_{\mathbf{L}} = \emptyset$, so the conditions (011), (101), and (110) correspond to medial checkerboard antidirections. We will consider the directions first.

5.3 Medial checkerboard directions and Fano properties

We begin by considering condition (100). Much of the work is done by the following lemma.

Lemma 5.7. *Let $\boldsymbol{G}$ be a graph embedding with medial checkerboard $\mathbf{M}$ and jewel $\mathbf{L}$. Let δ be a bidirection of M and $\lambda = \tau(\delta)$ the corresponding binary labeling of $\mathbf{L}$. Then δ is a c-direction of $\mathbf{M}$ if and only if λ is an $E_{\mathbf{L}}^{\mathsf{fza}}$-labeling of $\mathbf{L}$.*

Proof. We reason as follows.

Under δ every edge of M is directed and every edge of $\boldsymbol{G}$ is a c-edge.
$\Leftrightarrow$ Under δ every edge of $\mathbf{M}$ is directed, and around a vertex the cyclic order of edge directions and face colors is (in (towards the vertex), v, in, f, out, v, out, f).
$\Leftrightarrow$ (Observation 5.6) Under δ_L each edge of color a in $\mathbf{L}$ is directed, and around an e-square of $\mathbf{L}$ the cyclic order of directions of incident half-edges and edge colors is (in (towards the e-square), v, in, f, out, v, out, f).
$\Leftrightarrow$ The binary labeling $\lambda = \tau(\delta)$ of L changes value across edges of color a in $\mathbf{L}$, and around an e-square of $\mathbf{L}$ the cyclic order of label values and edge colors is (0, v, 0, f, 1, v, 1, f). so that values change across edges of colors f and z, but do not change across edges of color v.
$\Leftrightarrow$ λ is an $E_{\mathbf{L}}^{\mathsf{fza}}$-labeling of $\mathbf{L}$. □

Theorem 5.8. *Let $\boldsymbol{G}$ be a graph embedding with medial checkerboard $\mathbf{M}$. Then $\boldsymbol{G}$ satisfies condition (100), i.e., $\boldsymbol{G}^{*\times}$ and $\boldsymbol{G}^{*\times *}$ are orientable, if and only if there is a c-direction of $\mathbf{M}$. Such a direction is a balanced direction, and is unique up to reversal on components of M.*

Proof. Let $\mathbf{L}$ be the jewel of $\boldsymbol{G}$. By Lemma 5.7 there is a c-direction δ of $\mathbf{M}$ if and only if $\mathbf{L}$ has an $E_{\mathbf{L}}^{\mathsf{fza}}$-labeling $\lambda = \tau(\delta)$, which by Table 1 is true if and only if $\boldsymbol{G}$ satisfies condition (100).

If δ exists, it is a balanced direction by Observation 5.5. There are two choices for directing the edges incident with a given vertex v_e of $\mathbf{M}$ so that v_e is a c-vertex, which are reverses of each other. But once we choose one of these we fix the choice at all neighbors of v_e, and by propagation, at all vertices in the same component as v_e. Thus, δ is unique up to reversal on components of M. □

We can also begin with a 4-regular graph M with a balanced direction δ, and ask whether we can embed and face-color M to obtain a medial checkerboard with a bidirection as in Theorem 5.8, corresponding to an embedded graph $\boldsymbol{G}$ for which condition (100) holds. In general we obtain many such $\boldsymbol{G}$.

Theorem 5.9. *Let M be a 4-regular graph with a balanced direction δ. We can embed and face-color M to obtain at least one medial checkerboard $\mathbf{M}$ in which every vertex of $\mathbf{M}$ is a c-vertex under δ. The medial checkerboards $\mathbf{M}$ obtainable in this way correspond to an equivalence class $\mathcal{G}$ of embedded graphs under partial Petrie duality. Any other bidirected 4-regular graph that corresponds to $\mathcal{G}$ in this way is isomorphic to M with a bidirection obtained from δ by reversal on a subset of components of M.*

Proof. Create a new 4-regular graph L from M by expanding each vertex v of M to a copy T_v of K_4 (a *simplex*), so that each edge of M incident with v becomes incident with a distinct vertex of T_v in L. Then L has the structure of the underlying graph of a jewel, and $M = L \phi S$ where S is the set of simplex edges. We can obtain a binary labeling $\lambda = \tau(\delta)$ of L from δ in the manner described earlier for checkerboards and jewels, with an intermediate bidirection δ_L of $A = E(L) - S$.

In each T_v two vertices will be labeled 0 and two vertices will be labeled 1. Color the edges of A in L with a, and color the two edges of each simplex with equal labels on their endvertices with v. The remaining four edges of the simplex form two matchings: color the edges of one matching with f and the edges of the other with z. The result is a jewel $\mathbf{L}$ for which λ is a $E_{\mathbf{L}}^{\mathsf{fza}}$-labeling, corresponding to an embedded graph $\boldsymbol{G}$ satisfying condition (100). Since $M = L \phi E_{\mathbf{L}}^{\mathsf{vfz}}$, M is the medial graph of $\boldsymbol{G}$, and so the medial checkerboard $\mathbf{M}$ of $\boldsymbol{G}$ is obtained by embedding and face-coloring M. Now δ is a bidirection of $\mathbf{M}$ and $\lambda = \tau(\delta)$ is an $E_{\mathbf{L}}^{\mathsf{fza}}$-labeling of $\mathbf{L}$. Thus, by Lemma 5.7, every edge of $\boldsymbol{G}$ is a c-edge under δ, as required.

This construction allows us to swap the colors f and z on any simplices of $\mathbf{L}$, which corresponds to taking arbitrary partial Petrie duals of $\boldsymbol{G}$, forming an equivalence class $\mathcal{G}$. Any $\boldsymbol{G} \in \mathcal{G}$ determines M, and by Theorem 5.8 it also determines δ up to reversal on components of M. □

Every 4-regular graph has a balanced direction (take an Euler circuit T and direct every edge in the direction of T), so the proof of Theorem 5.9 gives a method for constructing graph embeddings with a given medial graph M and satisfying condition (100). Also, note that two embedded graphs in the class $\mathcal{G}$ from Theorem 5.9 always have the same medial graph M, but their medial embeddings $\boldsymbol{M}$ will usually be distinct.

We can apply similar analyses to conditions (001) and (010). We omit the proofs, but state the results in Theorems 5.10 and 5.11 below.

The fourth condition related to a medial checkerboard direction is condition (111). This is equivalent to $\mathbf{M}$, or M, being bipartite. While an argument using an $E^{\mathsf{a}}_{\mathbf{L}}$-labeling of $\mathbf{L}$ can be made, it is easy to see directly that this is equivalent to $\mathbf{M}$ having a bidirection in which every edge of $\boldsymbol{G}$ is a t-edge: the bipartition of $\mathbf{M}$ is just the partition into t^+- and t^--vertices. For the counterpart of Theorem 5.9 for condition (111), we create a jewel $\mathbf{L}$ with an $E^{\mathsf{a}}_{\mathbf{L}}$-labeling based on a total direction of M. In any given simplex, all vertices have the same label, and we can color the three matchings in the simplex arbitrarily with the colors $\mathsf{v}, \mathsf{f}, \mathsf{z}$. We can permute these colors arbitrarily on each simplex, which corresponds to taking arbitrary twisted duals of $\boldsymbol{G}$.

The results for all four conditions (001), (010), (100), and (111) can be summarized by the following two theorems, which refer to Table 3.

Theorem 5.10. *Let $\boldsymbol{G}$ be a graph embedding with medial checkerboard $\mathbf{M}$ and jewel $\mathbf{L}$. Choose γ, σ, S and (β) from the same row of Table 3.*

(a) *Let δ be a bidirection of M and $\lambda = \tau(\delta)$ the corresponding binary labeling of L. Then δ is a σ-direction of $\mathbf{M}$ if and only if λ is an S-labeling of $\mathbf{L}$.*

(b) *Condition (β) holds for $\boldsymbol{G}$ if and only if there is a σ-direction of $\mathbf{M}$. Such a direction is a direction of general type γ, and is unique up to reversal on components of M.*

Direction of $\mathbf{M}$				
General type γ	Specific type σ	S-labeling of $\mathbf{L}$	Condition (β) and property of $\boldsymbol{G}$	Operation class $\mathcal{O}$ defining $\mathcal{G}$
balanced	b	$E^{\mathsf{vfa}}_{\mathbf{L}}$-labeling	condition (001), i.e., $\boldsymbol{G}$, $\boldsymbol{G}^*$ orientable	partial duality
balanced	c	$E^{\mathsf{fza}}_{\mathbf{L}}$-labeling	condition (100), i.e., $\boldsymbol{G}^{*\times}$, $\boldsymbol{G}^{*\times *}$ orientable	partial Petrie duality
balanced	d	$E^{\mathsf{vza}}_{\mathbf{L}}$-labeling	condition (010), i.e., $\boldsymbol{G}^{\times}$, $\boldsymbol{G}^{\times *}$ orientable	partial Wilson duality
total	t	$E^{\mathsf{a}}_{\mathbf{L}}$-labeling	condition (111), i.e., $\mathbf{M}$ bipartite	twisted duality

Table 3: Correspondences for Theorems 5.10 and 5.11.

Theorem 5.11. *Choose γ, σ, (β), and $\mathcal{O}$ from the same row of Table 3. Let M be a 4-regular graph with a direction δ of general type γ; M always has such a direction if γ is 'balanced'.*

We can embed and face-color M to obtain at least one medial checkerboard $\mathbf{M}$ in which δ is a σ-direction, i.e., so that condition (β) holds for the corresponding embedded graph $\boldsymbol{G}$. The medial checkerboards $\mathbf{M}$ obtainable in this way correspond to an equivalence class $\mathcal{G}$ of embedded graphs under the operations in $\mathcal{O}$. Any other bidirected 4-regular graph that corresponds to $\mathcal{G}$ in this way is isomorphic to M with a bidirection obtained from δ by reversal on a subset of components of M.

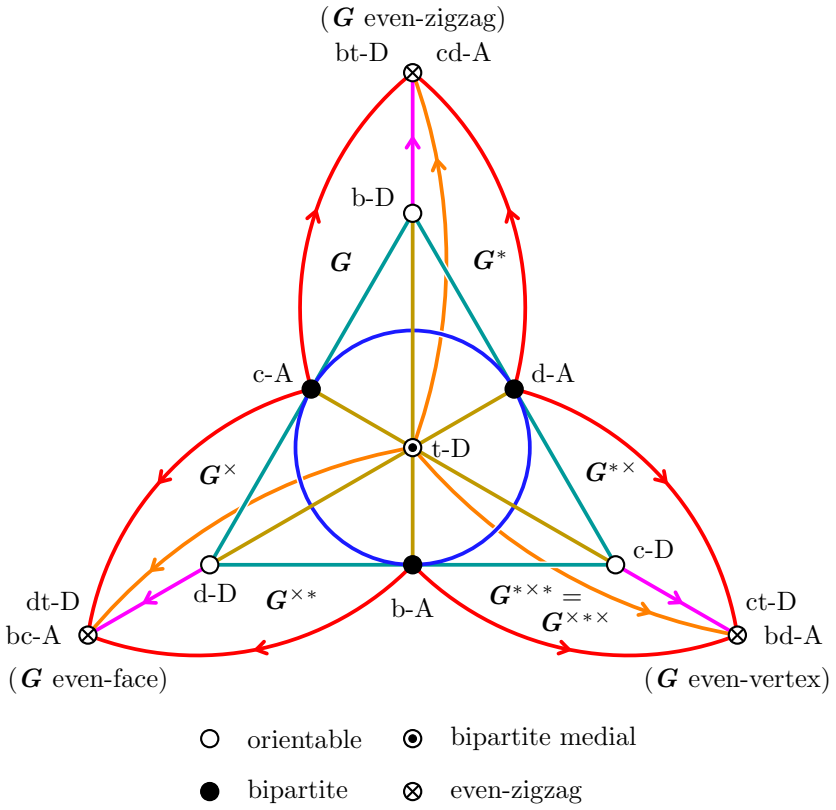

Figure 7: Extended Fano Framework (D = direction, A = antidirection).

The results summarized in Theorems 5.10 and 5.11 are, as far as we are aware, new, except for part of the result for d-directions, stated earlier as Theorem 5.4, due to Yan and Jin. In particular, there are no prior results involving b-edges.

There are other ways to prove some of these results, as we already noted above for condition (111). For example, we can show that if $\boldsymbol{G}$ is orientable, then there is a b-direction of $\mathbf{M}$: just choose one color, either v or f, and direct all faces of $\boldsymbol{M}$ of that color in the clockwise direction for some orientation of the surface. Yan and Jin used a similar argument to prove Theorem 5.4. Conversely, we can apply Theorem 3.12 to the medial embedding $\boldsymbol{M}$ to show that if there is a b-direction of $\mathbf{M}$, then $\boldsymbol{M}$, and hence $\boldsymbol{G}$, is orientable.

We have now associated four of the seven Fano framework properties with a property involving medial graph directions. These results are indicated on Figure 7, an extended version of Figure 5. Each of the central vertex and the open vertices is marked with the type of direction that characterizes its property. For example, the top open vertex is marked with 'b-D' to indicate that its property, orientability of $\boldsymbol{G}$ or $\boldsymbol{G}^*$, corresponds to existence of a b-direction of $\mathbf{M}$. Other parts of Figure 7 will be explained later.

5.4 Twisted duality and balanced-total bidirections

We next characterize the effect of partial duality and partial Petrie duality on edge types for a bidirection δ of the medial graph M of an embedded graph $\boldsymbol{G}$. As noted in Subsection 5.3, a twisted duality operation does not change δ or the corresponding labeling $\lambda = \tau(\delta)$ of the underlying graph L of the jewel. However, the types of vertices of the medial checkerboard may change. Observation 5.6(c) allows us to transfer information about changes in the jewel to information about vertex types in the medial checkerboard, i.e. edge types in the embedded graph.

Theorem 5.12. *Suppose we have an embedded graph $\boldsymbol{G}$, a fixed balanced-total bidirection δ of its medial graph M, and $A \subseteq E(G)$. In the partial dual $\boldsymbol{G} * A$, or partial Petrie dual $\boldsymbol{G} \times A$, the type of each edge of $\boldsymbol{G}$ not in A does not change, and the type of each edge in A changes according to Table 4.*

Effect on edges in A		
Type in $\boldsymbol{G}$	Type in $\boldsymbol{G} * A$	Type in $\boldsymbol{G} \times A$
b-edge	b-edge	d-edge
c-edge	d-edge	c-edge
d-edge	c-edge	b-edge
t^+-edge	t^+-edge	t^+-edge
t^--edge	t^--edge	t^--edge

Table 4: Type changes under partial duality and partial Petrie duality.

Proof. We examine one case; the others are similar. Let $\mathbf{L}$ be the jewel of $\boldsymbol{G}$, and $\delta_{\mathbf{L}}$ the bidirection of $E^{\mathsf{a}}_{\mathbf{L}}$ corresponding to $\delta_{\mathbf{M}}$. Suppose $e \in A$ is a b-edge in $\boldsymbol{G}$, corresponding to an e-simplex in $\mathbf{L}$ containing the e-square $\mathbf{Q}_e = (u_0u_1u_2u_3)$. Applying Observation 5.6, we may assume that edges u_0u_1 and u_2u_3 are colored v, edges u_1u_2 and u_3u_0 are colored f, and under $\delta_{\mathbf{L}}$ edges of $E^{\mathsf{a}}_{\mathbf{L}}$ are directed into u_0 and u_2, and out of u_1 and u_3. In the jewel $\mathbf{L}[\times A]$ of $\boldsymbol{G} \times A$, the colors f and z are swapped on the e-simplex, and the e-square of the recolored e-simplex is $\mathbf{Q}'_e = (u_0u_1u_3u_2)$, where u_0u_1 and u_2u_3 are still colored v, while u_1u_3 and u_0u_2 are colored f. Therefore, around $\mathbf{Q}'_e$ we have (in (u_0), f, in (u_2), v, out (u_3), f, out (u_1), v). Applying Observation 5.6, we see that e is now a d-edge. □

A special case of Theorem 5.12 was given by Deng, Jin, and Metsidik [13, Lemma 2.4]. They showed that under full duality all c-edges become d-edges, and vice versa, while t-edges remain t-edges.

Using Theorem 5.12 we can track the effect on edge types (relative to a fixed medial graph direction) for any sequence of partial dual and partial Petrie dual operations. This has many consequences; we provide a few examples.

(1) Taking the partial Wilson dual with respect to A, $\boldsymbol{G} \mapsto \boldsymbol{G} \times * \times A = \boldsymbol{G} \odot A$, interchanges b- and c-edges for edges in A and leaves other edges and types unchanged.

(2) The operation $\boldsymbol{G} \mapsto \boldsymbol{G} * A \times B$ permutes the edge type as (bdc) for edges in $A \cap B$ (b-edges become d-edges, d-edges become c-edges, c-edges become b-edges), as (cd) for edges in $A - B$, and as (bd) for edges in $B - A$.

(3) An alternative way to prove the parts of Theorems 5.10 and 5.11 for b- and d-directions is to derive them from c-direction results (Lemma 5.7 and Theorems 5.8 and 5.9) by using Theorem 5.12 (possibly more than once) with $A = E(G)$.

(4) We can prove results of the same flavor as Theorems 5.2 and 5.3, characterizing when an embedded graph has a particular type of twisted dual that is orientable. The conditions for an orientable partial dual may be summarized as follows.

Theorem 5.13. *Let $\boldsymbol{G}$ be an embedded graph with medial checkerboard $\mathbf{M}$. Then a twisted dual of $\boldsymbol{G}$ is orientable if and only if there exists a direction of $\mathbf{M}$ satisfying the following conditions.*

(i) *The edges of $\boldsymbol{G}$ that are unchanged or operated on by $*$ are b-edges,*

(ii) *the edges of $\boldsymbol{G}$ that are operated on by $*\times$ or $* \times *$ are c-edges, and*

(iii) *the edges of $\boldsymbol{G}$ operated on by $\times$ or $\times*$ are d-edges.*

Proof. Let $\boldsymbol{G}'$ be the twisted dual. If we have a balanced direction of $\mathbf{M}$ satisfying the above conditions, then by Theorem 5.12 all edges become b-edges after taking the twisted dual, so by Theorem 5.10 $\boldsymbol{G}'$ is orientable. Conversely, if $\boldsymbol{G}'$ is orientable then there is a b-direction of its medial checkerboard $\mathbf{M}'$, and after reversing the twisted dual we see that the edges of $\boldsymbol{G}$ have the specified types. □

(5) We see that Theorem 5.3, and its special case Theorem 5.2, regarding bipartiteness of partial duals, are really a combination of three separate ideas. First, an orientable embedded graph $\boldsymbol{G}$ is bipartite if and only if $\boldsymbol{G}^\times$ is orientable, which is part of the Fano framework. Second, $\boldsymbol{G}^\times$ is orientable if and only if $\boldsymbol{G}$ has a medial checkerboard direction where every edge of $\boldsymbol{G}$ is a d-edge, by Theorem 5.10. And third, partial duality interchanges c-edges and d-edges in the dualized set of edges, by Theorem 5.12. We will see a more direct way to address bipartiteness in Subsection 5.5.

5.5 Medial checkerboard antidirections and Fano properties

As noted at the end of Subsection 5.2, conditions for an embedded graph $\boldsymbol{G}$ involving an S-labeling of the jewel $\mathbf{L}$ where $S \cap E^{\mathsf{a}}_{\mathbf{L}} = \emptyset$ correspond to antidirections of the medial checkerboard. Here we consider b-, c-, and d-antidirections of $\mathbf{M}$. We could also consider t-antidirections, but every medial checkerboard has a t-antidirection obtained by antidirecting each edge in the same way (all introverted, or all extraverted). Thus, the existence of a t-antidirection corresponds to the always-true condition (000).

We can apply the same type of analysis to b-, c-, and d-antidirections of $\mathbf{M}$ that we applied to b-, c-, and d-directions of $\mathbf{M}$ in Subsection 5.3. The arguments are very similar. For example, we saw that a c-direction of $\mathbf{M}$ corresponds to an $E^{\mathsf{fza}}_{\mathbf{L}}$-labeling of $\mathbf{L}$. By much the same reasoning, a c-antidirection of $\mathbf{M}$ corresponds to an $E^{\mathsf{fz}}_{\mathbf{L}}$-labeling of $\mathbf{L}$. The results for b-, c-, and d-antidirections and the respective three conditions (110), (011), and (101) can be summarized by Theorems 5.14 and 5.15, which refer to Table 5. Since the proofs are very similar to those of Theorems 5.10 and 5.11, we omit them, apart from a discussion of the existence of balanced antidirections before Theorem 5.15.

Theorem 5.14. *Let $\boldsymbol{G}$ be a graph embedding with medial checkerboard $\mathbf{M}$ and jewel $\mathbf{L}$. Choose γ, σ, S and (β) from the same row of Table 5.*

(a) *Let δ be a bidirection of M and $\lambda = \tau(\delta)$ the corresponding binary labeling of L. Then δ is a σ-antidirection of $\mathbf{M}$ if and only if λ is an S-labeling of $\mathbf{L}$.*

(b) *Condition (β) holds for $\boldsymbol{G}$ if and only if there is a σ-antidirection of $\mathbf{M}$. Such an antidirection is an antidirection of general type γ (here, always balanced), and is unique up to reversal on components of $\mathbf{M}$.*

Antidirection of $\mathbf{M}$				
General type γ	Specific type σ	S-labeling of $\mathbf{L}$	Condition (β) and property of $\boldsymbol{G}$	Operation class $\mathcal{O}$ defining $\mathcal{G}$
balanced	b	$E^{\mathsf{vf}}_{\mathbf{L}}$-labeling	condition (110), i.e., $\boldsymbol{G}^{\times *}$, $\boldsymbol{G}^{*\times *}$ bipartite	partial duality
balanced	c	$E^{\mathsf{fz}}_{\mathbf{L}}$-labeling	condition (011), i.e., $\boldsymbol{G}$, $\boldsymbol{G}^\times$ bipartite	partial Petrie duality
balanced	d	$E^{\mathsf{vz}}_{\mathbf{L}}$-labeling	condition (101), i.e., $\boldsymbol{G}^*$, $\boldsymbol{G}^{*\times}$ bipartite	partial Wilson duality

Table 5: Correspondences for Theorems 5.14 and 5.15.

Every 4-regular graph M has an even number of edges, and therefore, by designating edges as introverted or extraverted in an alternating way as we follow an Euler circuit in M, we see that M has at least one balanced antidirection. Thus, we can use reasoning similar to that of Theorem 5.9 and the associated discussion to construct graph embeddings with a given medial graph M and satisfying one of the conditions (011), (101) or (110).

Theorem 5.15. *Choose γ, σ, (β), and $\mathcal{O}$ from the same row of Table 5. Let M be a 4-regular graph with an antidirection δ of general type γ (here, always balanced); M always has such an antidirection.*

We can embed and face-color M to obtain at least one medial checkerboard $\mathbf{M}$ in which δ is a σ-antidirection, i.e., so that condition (β) holds for the corresponding embedded graph $\boldsymbol{G}$. The medial checkerboards $\mathbf{M}$ obtainable in this way correspond to an equivalence class $\mathcal{G}$ of embedded graphs under the operations in $\mathcal{O}$. Any other bidirected 4-regular graph that corresponds to $\mathcal{G}$ in this way is isomorphic to M with a bidirection obtained from δ by reversal on a subset of components of M.

The results summarized in Theorems 5.14 and 5.15 are, as far as we are aware, new.

We have now associated three of the seven Fano framework properties with a property involving medial graph antidirections. Each solid vertex of Figure 7 is marked with the type of antidirection that characterizes its property. For example, the solid vertex on the left is marked with 'c-A' to indicate that its property, bipartiteness of $\boldsymbol{G}$ or $\boldsymbol{G}^{\times}$, corresponds to existence of a c-antidirection of $\mathbf{M}$.

Antidirections of M are really just binary labelings of the edges of M (e.g., extraverted edges are 0, introverted edges are 1). We can also think of them as signings of the edges (e.g., extraverted edges are $-$, introverted edges are $+$) or as colorings of the edges (e.g., extraverted edges are black, introverted edges are white).

Thinking of antidirections as colorings gives more intuitive proofs of Theorem 5.14. For example, if we think of a c-antidirection of $\mathbf{M}$ as a black/white coloring of the edges of $\mathbf{M}$, the monochrome cycles in $\mathbf{M}$ are precisely the boundaries of the faces of $\mathbf{M}$ colored v, and each vertex v_e is contained in both a black cycle and a white cycle. In other words, we have a black/white coloring of the vertices of $\boldsymbol{G}$, and each edge e of $\boldsymbol{G}$ joins a black vertex and a white vertex, meaning that $\boldsymbol{G}$ is bipartite.

Theorem 5.12 applies to antidirections of the medial graph, as well as to directions. We can use this in conjunction with Theorem 5.14 to give a general characterization of embedded graphs with bipartite twisted duals, similar to the characterization of orientable twisted duals in Theorem 5.13. Unlike Theorems 5.2 and 5.3, it uses antidirections, rather than directions, of the medial checkerboard, it applies to nonorientable embeddings as well as orientable embeddings, and it applies to all twisted duals, not just partial duals.

Theorem 5.16. *Let $\boldsymbol{G}$ be an embedded graph with medial checkerboard $\mathbf{M}$. Then a twisted dual of $\boldsymbol{G}$ is bipartite if and only if there exists an antidirection of M satisfying the following conditions.*

(i) *The edges of $\boldsymbol{G}$ that are unchanged or operated on by $\times*$ or $*\times*$ are b-edges,*

(ii) *the edges of $\boldsymbol{G}$ that are unchanged or operated on by $\times$ are c-edges, and*

(iii) *the edges of $\boldsymbol{G}$ operated on by $*$ or $*\times$ are d-edges.*

Proof. Let $\boldsymbol{G}'$ be the twisted dual. If we have a balanced antidirection of M satisfying the above conditions, then by Theorem 5.12 all edges become c-edges after taking the twisted dual, so by Theorem 5.10 $\boldsymbol{G}'$ is bipartite. Conversely, if $\boldsymbol{G}'$ is orientable then there is a c-antidirection of its medial checkerboard $\mathbf{M}'$, and after reversing the twisted dual we see that the edges of $\boldsymbol{G}$ have the specified types. □

We can state similar results for twisted duals that are 2-face-colorable or 2-zigzag-colorable; we leave the details to the reader. Theorem 5.16 and these related results allow us to answer a question of Ellis-Monaghan and Moffatt [16, (1), pp. 1566-1567], as to which graph embeddings have a checkerboard colorable (i.e., 2-face-colorable) or bipartite twisted dual.

Corollary 5.17. *Every embedded graph $\boldsymbol{G}$ has a twisted dual that is bipartite, a twisted dual that is 2-face-colorable, and a twisted dual that is 2-zigzag-colorable.*

Proof. Construct an arbitrary balanced antidirection δ of the medial graph M of $\boldsymbol{G}$, which we know exists. Then apply a twisted dual operation to the edges of $\boldsymbol{G}$ following the specifications in Theorem 5.16(i)–(iii). The result is a bipartite twisted dual of $\boldsymbol{G}$. Twisted duals that are 2-face-colorable or 2-zigzag-colorable can be found in similar ways. □

6 Eulerian properties

In this subsection we consider the property of being Eulerian, or more generally even-vertex, for an embedded graph $\boldsymbol{G}$. (In the literature in this area, 'Eulerian' is often used to mean 'even-vertex', but we reserve 'Eulerian' for connected graphs.) We also consider the related properties of being even-face or even-zigzag. We will henceforth refer to the properties even-vertex, even-face, and even-zigzag as *Eulerian properties*. The Eulerian properties are weaker than the seven Fano properties, in the following way. Each of the seven properties implies at least one of these three new properties (as we show in this section), but $\boldsymbol{G}$ may have all three new properties and none of the seven properties (as demonstrated later by an example).

We will find several ways to characterize the three Eulerian properties. First we discuss how these properties can be represented in terms of parity conditions on closed walks. Then we show that these properties can be described in terms of both directions and antidirections of the medial graph. These descriptions allow us to show that each of the seven Fano properties implies one, two, or all three of the Eulerian properties.

6.1 Parity conditions for 2-color walks

To extend the idea of considering the parity of closed walks in a gem or jewel to cover the Eulerian properties, we must restrict the closed walks we consider to 2-*color* walks, which use edges of only two colors (any two colors are allowed).

To consider parity conditions for sets of edges in 2-color closed walks, by Theorem 3.4 we may restrict our attention to 2-color cycles. These are the v-gons, f-gons, and e-squares of a gem $\mathbf{J}$ or jewel $\mathbf{L}$, and for $\mathbf{L}$ also the z-gons, the 4-cycles of color v and z, and the 4-cycles of color f and z. All 4-cycles K using two of the colors $\mathsf{v}, \mathsf{f}, \mathsf{z}$ in either $\mathbf{J}$ or $\mathbf{L}$ use an even number of edges of each of the four colors $\mathsf{v}, \mathsf{f}, \mathsf{z}, \mathsf{a}$, so we may ignore these and consider only the v-gons, f-gons, and (for $\mathbf{L}$) z-gons. The degree of a vertex of $\boldsymbol{G}$ is the number of edges colored v in the corresponding v-gon, or equivalently the number of edges colored a in that v-gon.

We can describe all three Eulerian properties using conditions on 2-color walks in the jewel, but only two of them using such conditions for the gem. We describe the conditions for the jewel first.

The proposition below characterizes when we have one, two, or all three of the Eulerian properties. It partly follows from the comments in the previous paragraph. To obtain the final part of each of (a), (b), or (c), we recall that all closed 2-color walks have even length, so the number of edges of a given color is even if and only if the number of edges not of that color is even.

Proposition 6.1. *Let $\boldsymbol{G}$ be an embedded graph with jewel $\mathbf{L}$.*

(a) *$\boldsymbol{G}$ is even-vertex if and only if $v_{\mathbf{L}}(K)$ is even for all 2-color closed walks K in $\mathbf{L}$ if and only if $(f+z+a)_{\mathbf{L}}(K)$ is even for all 2-color closed walks in $\mathbf{L}$.*

(b) *$\boldsymbol{G}$ is both even-vertex and even-face if and only if $(v+f)_{\mathbf{L}}(K)$ is even for all 2-color closed walks K in $\mathbf{L}$ if and only if $(z+a)_{\mathbf{L}}(K)$ is even for all 2-color closed walks K in $\mathbf{L}$.*

(c) *$\boldsymbol{G}$ is even-vertex, even-face, and even-zigzag if and only if $(v+f+z)_{\mathbf{L}}(K)$ is even for all 2-color closed walks K in $\mathbf{L}$ if and only if $a_{\mathbf{L}}(K)$ is even for all 2-color closed walks K in $\mathbf{L}$.*

We can permute the colors to obtain a condition for even-face embeddings or even-zigzag embeddings from (a), and a condition for even-vertex and even-zigzag, or even-face and even-zigzag, embeddings from (b). Therefore, each Eulerian property, and each nonempty combination of those properties, can be checked using a single parity condition for 2-color walks in the jewel.

If we work with the gem $\mathbf{J}$ instead of the jewel $\mathbf{L}$, we have the following.

Proposition 6.2. *Let $\boldsymbol{G}$ be an embedded graph with gem $\mathbf{J}$.*

(a) *$\boldsymbol{G}$ is even-vertex if and only if $v_{\mathbf{J}}(K)$ is even for all 2-color closed walks K in $\mathbf{J}$ if and only if $(f + a)_{\mathbf{J}}(K)$ is even for all 2-color closed walks in $\mathbf{J}$.*

(b) *$\boldsymbol{G}$ is both even-vertex and even-face if and only if $(v + f)_{\mathbf{J}}(K)$ is even for all 2-color closed walks K in $\mathbf{J}$ if and only if $a_{\mathbf{J}}(K)$ is even for all 2-color closed walks K in $\mathbf{J}$.*

We can permute the colors to obtain a condition for even-face embeddings from (a). However, we cannot obtain conditions involving the even-zigzag property by using 2-color walks in $\mathbf{J}$.

Proposition 6.1 tells us that certain Eulerian properties follow from the seven Fano properties, because if a particular parity condition holds for all closed walks in $\mathbf{L}$, it certainly holds for the 2-color closed walks in $\mathbf{L}$. We can deduce the following. We already proved (a) directly when examining condition (100) in Subsubsection 4.2.3, and as noted earlier, this was observed by Lins [25, Theorem 2.9(b)].

Corollary 6.3. *Let $\boldsymbol{G}$ be an embedded graph.*

(a) *If condition (100) holds for $\boldsymbol{G}$, i.e., $\boldsymbol{G}^{*\times}$ and $\boldsymbol{G}^{*\times *}$ are orientable, then $\boldsymbol{G}$ is even-vertex.*

(b) *If condition (110) holds for $\boldsymbol{G}$, i.e., $\boldsymbol{G}^{\times *}$ and $\boldsymbol{G}^{*\times *}$ are bipartite, then $\boldsymbol{G}$ is both even-vertex and even-face.*

(c) *If condition (111) holds for $\boldsymbol{G}$, i.e., the medial graph M of $\boldsymbol{G}$ is bipartite, then $\boldsymbol{G}$ is even-vertex, even-face, and even-zigzag.*

Proof. (a) If condition (100) holds, then $(v + f + a)_{\mathbf{L}}(K)$ is even for all closed walks K, and hence for 2-color K; therefore $\boldsymbol{G}$ is even-vertex by Proposition 6.1(a).

The proofs of (b) and (c) are similar: for (b) we use the function $(v + f)_{\mathbf{L}}$, and for (c) we use the function $a_{\mathbf{L}}$. (Each part of Proposition 6.1 gives two functions; from Subsection 3.4) we see that only one corresponds to a Fano condition.) □

By permuting colors in the jewel we can find eulerian properties implied by all seven Fano properties. The implications are shown in Figure 7. We will prove these implications again using bidirections of the medial graph, in the next subsection.

6.2 Medial graph bidirections and Eulerian properties

Huggett and Moffatt [23] considered not only the question of when a partial dual is bipartite, as described in Subsection 5.1, but also when it is Eulerian. They were able to give a sufficient condition [23, Corollary 4.5] involving directions of the medial checkerboard $\mathbf{M}$ for a partial dual of a plane graph to be Eulerian, but it was not a necessary condition (the condition was actually equivalent to $\boldsymbol{G}$ being 2-face-colorable). Metsidik and Jin [29] found a condition that was both necessary and sufficient, involving bidirections of $\mathbf{M}$ with both directed and antidirected edges. These bidirections had c- and d-edges and satisfied additional conditions. Metsidik [28] generalized this result, using similar bidirections with c-, d-, and t-edges to characterize when the partial dual of an arbitrary graph embedding is even-vertex. (Note that [28] employs nonstandard terminology, using 'c-edge' to mean either c- or t-edge, and 'd-edge' to mean either d- or t-edge.)

Deng, Jin, and Metsidik realized that simpler conditions could be given just using directions of $\mathbf{M}$, as follows.

Theorem 6.4 (Deng, Jin, and Metsidik [13, Theorem 1.5])**.** *Let $\boldsymbol{G}$ be a cellularly embedded graph with medial graph M and $A \subseteq E(\boldsymbol{G})$. Then $\boldsymbol{G} * A$ is even-vertex if and only if there exists a direction of M for which every element of A is a d-edge or a t-edge in $\boldsymbol{G}$, and every element of $E(G) - A$ is a c-edge or a t-edge in $\boldsymbol{G}$.*

By applying the special case of Theorem 5.12 for full duality, Deng, Jin, and Metsidik [13, Corollary 3.5] also obtained a condition for partial duals that are even-face. If we take $A = \emptyset$ or $A = E(G)$ in Theorem 6.4, we obtain the following.

Corollary 6.5. *Let **G** be a cellularly embedded graph with medial checkerboard* $\mathbf{M}$*. Then **G** is even-vertex if and only if there exists a ct-direction of* $\mathbf{M}$*.*

Corollary 6.6. *Let **G** be a cellularly embedded graph with medial checkerboard* $\mathbf{M}$*. Then **G** is even-face if and only if there exists a dt-direction of* $\mathbf{M}$*.*

In keeping with our theme of breaking results down to simpler components, we observe that Theorem 6.4 is just a consequence of Corollary 6.5 and Theorem 5.12. We can also use Theorem 5.12 to characterize the situation where $\mathbf{M}$ has a bt-direction.

Theorem 6.7. *Let **G** be a cellularly embedded graph with medial graph* M*. Then **G** is even-zigzag if and only if there exists a bt-direction of* $\mathbf{M}$*.*

Proof. The zigzag walks of $\boldsymbol{G}$ are the faces of $\boldsymbol{G}^\times$, so $\boldsymbol{G}$ is even-zigzag if and only if $\boldsymbol{G}^\times$ is even-face, which by Corollary 6.6 means the medial graph of $\boldsymbol{G}^\times$ has an orientation for which all edges of $\boldsymbol{G}^\times$ are d- or t-edges, which by Theorem 5.12 means all edges of $\boldsymbol{G}$ are b- or t-edges. □

Consequently, situations where we have a b-, c-, d-, or t-direction of the medial checkerboard $\mathbf{M}$, representing four of the properties in the Fano framework, imply that we have one or more of the properties even-vertex, even-face, or even-zigzag. For example, if we have conditions (001) or (111) we have a b-direction or a t-direction of $\mathbf{M}$, which in either case is a bt-direction, so by Theorem 6.7 $\boldsymbol{G}$ is even-zigzag. The implications are shown by directed edges (magenta or orange, if color is shown) in Figure 7. The results we obtain from this argument are the same as those we obtain from part (a), and its generalizations, and part (c) of Corollary 6.3.

Somewhat surprisingly, the Eulerian properties also correspond to combinations of antidirection properties, so we also get implications for the remaining three properties of the Fano framework, shown by directed edges (red, if color is shown) in Figure 7. We now prove the necessary results.

Theorem 6.8. *Let **G** be a cellularly embedded graph with medial checkerboard* $\mathbf{M}$*. Then **G** is even-vertex if and only if there exists a bd-antidirection of* $\mathbf{M}$*.*

Proof. Let $\mathbf{J}$ be the gem of $\boldsymbol{G}$.

First suppose $\boldsymbol{G}$ is even-vertex. Then we can antidirect the edges colored a in each v-gon of $\mathbf{J}$ so that they are alternately introverted and extraverted. Thus, each edge colored v in an e-square Q_e joins two half-edges of color a that have opposite directions relative to Q_e and so around Q_e we see either (in, v, out, f, in, v, out, f), or (in, v, out, f, out, v, in, f). By Observation 5.6, this means that e is either a b-edge or a d-edge in $\boldsymbol{G}$.

Conversely, suppose that $\mathbf{M}$ has a bd-antidirection. Then Observation 5.6 guarantees that each edge of color v in an e-square Q_e of $\mathbf{J}$ joins two half-edges of color a that have opposite directions relative to Q_e. Therefore, around each v-gon of J the edges of color a must alternate between introverted and extraverted, and hence each vertex of $\boldsymbol{G}$ has even degree. □

By applying Theorem 5.12 to Theorem 6.8 we obtain the following.

Theorem 6.9. *Let **G** be a cellularly embedded graph with medial checkerboard* $\mathbf{M}$*. Then **G** is even-face if and only if there exists a bc-antidirection of* $\mathbf{M}$*.*

Theorem 6.10. *Let **G** be a cellularly embedded graph with medial checkerboard* $\mathbf{M}$*. Then **G** is even-zigzag if and only if there exists a cd-antidirection of* $\mathbf{M}$*.*

Therefore, situations where we have a b-, c-, or d-antidirection of the medial checkerboard $\mathbf{M}$, representing the remaining three properties in the Fano framework, imply that we have two of the properties even-vertex, even-face, or even-zigzag. For example, if $\boldsymbol{G}$ satisfies condition (011), i.e., $\boldsymbol{G}$ and $\boldsymbol{G}^\times$ are bipartite, then $\mathbf{M}$ has a c-antidirection. Therefore, $\mathbf{M}$ has both a bc-antidirection and a cd-antidirection, meaning that $\boldsymbol{G}$ is both even-face and even-zigzag by Theorems 6.9 and 6.10. The implications we obtain in this way are identical to those given by part (b) of Corollary 6.3 and its generalizations.

At this point we can fully explain Figure 7. There are ten vertices, seven of which represent our Fano framework properties, and three new crossed vertices that represent Eulerian properties: whether the embedded graph $\boldsymbol{G}$ is even-vertex, even-face, or even-zigzag. The edges between the solid, open and crossed vertices (teal, magenta and red, if colors are shown) form six triangles, and each is labeled in its interior with an embedded graph $\boldsymbol{H}$ ($\boldsymbol{H} = \boldsymbol{G}$, $\boldsymbol{G}^*$, etc.). The open vertex of the triangle represents $\boldsymbol{H}$ being orientable, the solid vertex represents $\boldsymbol{H}$ being bipartite, and the crossed vertex represents $\boldsymbol{H}$ being even-zigzag (not the easiest property to interpret, but what makes the figure work nicely). For example, at top left is a triangle with the label '$\boldsymbol{G}$' inside it; the crossed vertex of this triangle represents $\boldsymbol{G}$ being even-zigzag; the open vertex represents $\boldsymbol{G}$ being orientable (condition (001)); and the solid vertex represents $\boldsymbol{G}$ being bipartite (condition (011)). The directed edges represent implications between properties, and the undirected edges represent the Fano framework, as in Figure 5.

We can combine the results above with Theorem 5.12 to obtain results about whether graphs obtained by taking an arbitrary sequence of partial duals and partial Petrie duals are even-vertex, even-face, or even-zigzag.

7 Examples

We now give examples of graph embeddings satisfying all possible combinations of the seven Fano properties. We will also provide an example to show that it is possible to have all three Eulerian properties without having any of the seven Fano properties.

Some of our examples are graphs embedded in the projective plane (represented as a disk with antipodal boundary points identified) or torus (represented as a rectangle with opposite sided identified). Other examples are represented as *rotation projections* in the plane: the graph is drawn in the plane so that the rotation at each vertex is just the clockwise cyclic order of half-edges; edges of signature -1 are marked with an X; and edge crossings should be ignored. Some examples are represented as rotation projections but in the torus rather than the plane.

7.1 Examples of allowable combinations of Fano properties

Here we provide examples showing that all combinations of Fano properties allowed by Metatheorem A actually occur.

7.1.1 All seven Fano properties

A grid embedding of $C_{2k} \times C_{2l}$ in the torus (Figure 8) satisfies all seven properties. It is orientable, bipartite, and 2-face-colorable. So the embedding satisfies conditions (001), (011), and (101), and by Metatheorem C all seven properties are satisfied.

7.1.2 Three Fano properties (side of triangle)

An embedding $\boldsymbol{G}$ of a tree with at least two vertices in the plane is orientable and bipartite (conditions (001) and (011)) so it also satisfies condition (010). However, the medial graph has a loop corresponding to each leaf of the tree, and hence is not bipartite. Since condition (111) does not hold, only the three conditions (001), (011), and (010) on the left side of the Fano triangle hold.

By taking the dual or the Wilson dual of such a $\boldsymbol{G}$ we obtain embeddings where exactly the three properties on one of the other two sides of the Fano triangle hold.

7.1.3 Three Fano properties (median of triangle)

Figure 9 shows an example where we have twisted one edge of a grid embedding of $C_{2k} \times C_{2l}$ in the torus, as illustrated in Figure 8, We keep the properties of being bipartite and having a bipartite medial graph

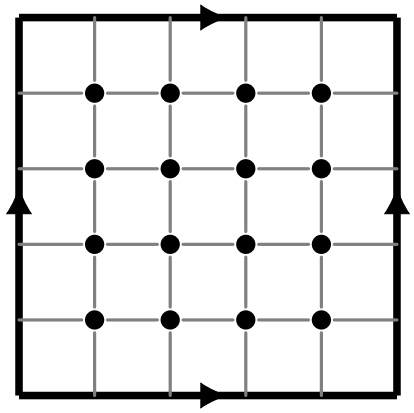

Figure 8: This embedding of $C_{2k} \times C_{2l}$ in the torus satisfies all seven properties.

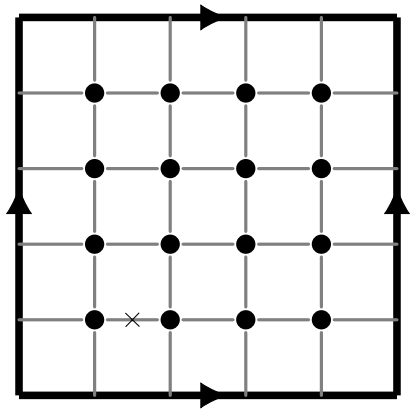

Figure 9: This embedding is bipartite (011) and the medial graph is bipartite (111), so we still have (100) as well, but this is not 2-face-colorable (101) so none of the other four properties can hold.

(conditions (011) and (111), which imply (100)) but lose 2-face-colorability (condition (101)). Therefore, only the three conditions (011), (111) and (100) hold in this case, representing the median of the Fano triangle from upper left to bottom right.

By taking the dual or Wilson dual of this embeddding we obtain embeddings where exactly the three properties on one of the other two medians of the Fano triangle hold.

7.1.4 Three Fano properties (circle)

Figure 10 shows an embedded graph $\boldsymbol{G}$ in the projective plane which is bipartite and 2-face-colorable (conditions (011) and (101), which imply condition (110)). However, this embedding is not orientable (condition (001)) and therefore it satisfies only the three conditions corresponding to the circular line of the Fano plane.

7.1.5 One Fano property (orientability)

In Figure 11 we give an embedding of K_4 in the plane that is such that neither the graph nor its dual are Eulerian (even-vertex). Therefore, it is orientable (condition (001)), but satisfies none of the other seven properties.

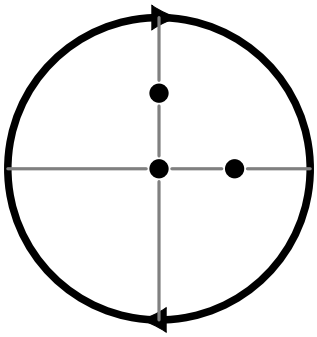

Figure 10: This graph drawn in the projective plane is bipartite, 2-face-colorable, but not orientable.

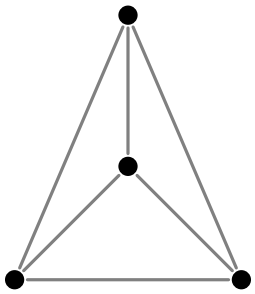

Figure 11: This embedding of K_4 in the plane satisfies only (001).

We can find examples that satisfy only condition (010) or only condition (100) by taking the Petrie dual or Wilson dual, respectively, of this example.

7.1.6 One Fano property (bipartiteness)

The embedding of $K_{3,3}$ in the projective plane shown in Figure 12 is bipartite, but it is not orientable, 2-face-colorable, or Eulerian (even-vertex). Thus, by Metatheorem B it only satisfies (011).

By taking a dual or Wilson dual of this example, we can find embeddings that satisfy only condition (101) or only condition (110), respectively.

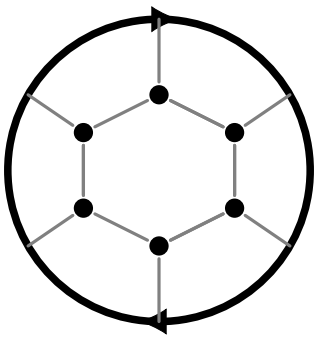

Figure 12: $K_{3,3}$ in the projective plane satisfies only (011).

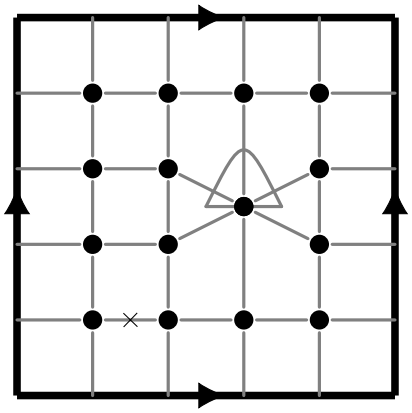

Figure 13: This partial twisted dual of $C_{2k} \times C_{2l}$ in the torus satisfies only (111).

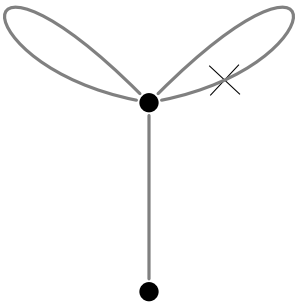

Figure 14: A graph G satisfying none of the ten properties.

7.1.7 One Fano property (medial graph is bipartite)

By taking a twisted dual of the graph in Figure 8, we can create the graph in Figure 13 which satisfies only (111). By taking the partial Petrie dual of one edge and the partial dual of another, the resulting graph in Figure 13 is not orientable, bipartite, or 2-face-colorable. The medial graph is still bipartite since twisted duality does not impact the underlying medial graph. Since the embedding satisfies (111) but not (001), (011), or (101), by Metatheorem B none of the other three conditions can be satisfied.

7.1.8 No Eulerian or Fano properties

The embedding in Figure 14 is not even-vertex (the vertex degrees are 5 and 1), not even-face (it has a face of degree 1), and not even-zigzag (it has a zigzag of degree 1). Since it has none of the Eulerian properties, it also has none of the Fano properties.

7.2 Example with all Eulerian properties but no Fano properties

In Subsubsection 7.1.8 above we provided an example with none of the seven Fano properties or three Eulerian properties. However, there are also examples showing that no combination of the Eulerian properties implies any of the Fano properties.

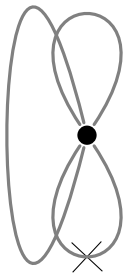

Figure 15: A graph G satisfying none of the fano properties but all three eulerian properties.

7.2.1 All Eulerian but no Fano properties

The embedding $\boldsymbol{G}$ in Figure 15 has a single vertex, a single face, and a single zigzag. Therefore, the vertex, face, and zigzag all have degree 6, and the embedding has all three Eulerian properties. However, because it has only a single vertex, single face, and single zigzag, it is not bipartite, 2-face-colorable, or 2-zigzag-colorable. The medial graph contains a triangle, so is not bipartite. Since $\boldsymbol{G}$ contains a twisted loop it is not orientable, and $\boldsymbol{G}^{\times}$ contains two twisted loops, so is not orientable. Finally, $\boldsymbol{G}$ is not directable: if we direct the edges so that each face is bounded by a directed walk, then the half-edge directions around the vertex would have to alternate between inward and outward, which is not possible.

8 Eulerian and single-vertex partial duals

In this section we discuss another property of embedded graphs that can be represented by a congruence condition involving closed walks in the jewel, and a strengthening of that property which we can also characterize.

8.1 Eulerian partial duals

A *vertex-face walk* in a jewel $\mathbf{L}$ is a closed walk that alternates between edges colored a and edges colored either v or f. A *vertex-face cycle* or *v/f-gon* in a jewel $\mathbf{L}$ is a cycle that alternates between edges colored a and edges colored either v or f. These v/f-gons represent a vertex (and equivalently a face) in some partial dual of the cellularly embedded graph $\boldsymbol{G}$ represented by $\mathbf{L}$.

Theorem 8.1. *Let $\boldsymbol{G}$ be a connected, cellularly embedded graph with corresponding jewel $\mathbf{L}$. All partial duals of $\boldsymbol{G}$ are Eulerian if and only if all v/f-gons have length 0 (mod 4).*

Proof. Let $\boldsymbol{G}$ be a connected, cellularly embedded graph with corresponding jewel $\mathbf{L}$. First assume that all partial duals of $\boldsymbol{G}$ are Eulerian. Then for any $A \subseteq E(G)$, the v-gons of $\mathbf{L}[*A]$ must have an even number of edges colored v. This means that the total length of the v-gon must be equal to 0 (mod 4). But, every v/f-gon in $\mathbf{L}$ represents a v-gon in $\mathbf{L}[*A]$ for some edge set $A \subseteq E(G)$. To see this, begin with a v/f-gon C in $\mathbf{L}$. Note that since C is a cycle, it cannot cross an e-square in $\mathbf{L}$ along both an edge colored v and an edge colored f. Using both an edge colored v and an edge colored f in the same e-square causes a vertex-face walk to use all three edges incident with a vertex, thus making it not a cycle. So, for each e-square e in $\mathbf{L}$, C crosses e along at most one color (it may use one or both edges of that color, but it may only use one of the two colors). Let A be the set of edges in $\boldsymbol{G}$ corresponding to e-squares in $\mathbf{L}$ that C crosses along edges colored f. Then consider $\boldsymbol{G} * A$. In $\boldsymbol{G} * A$, C becomes a v-gon since it is a v/f-gon with only edges colored a and v. Therefore C must have an even number of edges colored v since $\boldsymbol{G} * A$ is Eulerian by assumption and so C has length 0 (mod 4). Thus, all v/f-gons have length 0 (mod 4).

Conversely, assume that all v/f-gons have length 0 (mod 4). Let A be an arbitrarily chosen subset of $E(G)$. Let v be a vertex of $\boldsymbol{G} * A$. Then v is represented by a v-gon in $\boldsymbol{G} * A$ which is itself a v/f-gon in $\mathbf{L}$ up to possibly a different coloring on the edges colored v and f. The length of the v-gon representing v is 0 (mod 4) and thus v has even degree. Since v and A were chosen arbitrarily, we see that every vertex in a partial dual of $\boldsymbol{G}$ has even degree. Therefore, all partial duals of $\boldsymbol{G}$ are Eulerian. □

Corollary 8.2. *Let $\boldsymbol{G}$ be a connected, cellularly embedded graph with corresponding jewel $\mathbf{L}$. If for each cycle C in $\mathbf{L}$ either $(v+f)_{\mathbf{L}}(C)$ is even or $a_{\mathbf{L}}(C)$ is even, then all partial duals of $\boldsymbol{G}$ are Eulerian.*

Proof. Assume that $(v+f)_{\mathbf{L}}(C)$ is even or $a_{\mathbf{L}}(C)$ is even for all cycles C in $\mathbf{L}$. Then for each v/f-gon C in $\mathbf{L}$, since v/f-gons are themselves cycles in $\mathbf{L}$, $(v+f)_{\mathbf{L}}(C)$ or $a_{\mathbf{L}}(C)$ is even. However, in any v/f-gon $(v+f)_{\mathbf{L}}(C) = a_{\mathbf{L}}(C)$. Thus the total length of C is equal to 0 (mod 4). Therefore, by Theorem 8.1, all partial duals of $\boldsymbol{G}$ are Eulerian. □

Since the functions $(v+f)_{\mathbf{L}}$ and $a_{\mathbf{L}}$ correspond to conditions (110) and (111), respectively, we have the following.

Corollary 8.3. *Let $\boldsymbol{G}$ be a connected, cellularly embedded graph with corresponding medial graph M. If $\boldsymbol{G}$ is 2-zigzag-colorable or if M is bipartite then all partial duals of $\boldsymbol{G}$ are Eulerian.*

Note that the converse of Corollary 8.2 is not true. Figure 16 shows a counterexample. To simplify the figure we have shown only the gem $\mathbf{J}$, rather than the jewel $\mathbf{L}$; this still shows all of the v/f-gons. This connected graph has partial duals that have either a single vertex of degree 6 or two vertices of degree 4 and 2. So all partial duals are Eulerian, but in this graph there exists a cycle with $a_{\mathbf{J}}(C) = a_{\mathbf{L}}(C)$ odd and $(v+f)_{\mathbf{J}}(C) = (v+f)_{\mathbf{L}}(C)$ odd. One such cycle is $(0, 2, 3, 4, 8, 9, 10, 11)$ with three edges colored a, two edges colored f, and three edges colored v.

8.2 Single-vertex partial duals

We know that every connected graph embedding $\boldsymbol{G}$ has some Eulerian partial dual. In particular, it is well known that if T is the set of edges of a spanning tree in $\boldsymbol{G}$, then $\boldsymbol{G} * T$ has a single vertex. This vertex is incident with both ends of every edge, and thus $\boldsymbol{G} * T$ is Eulerian.

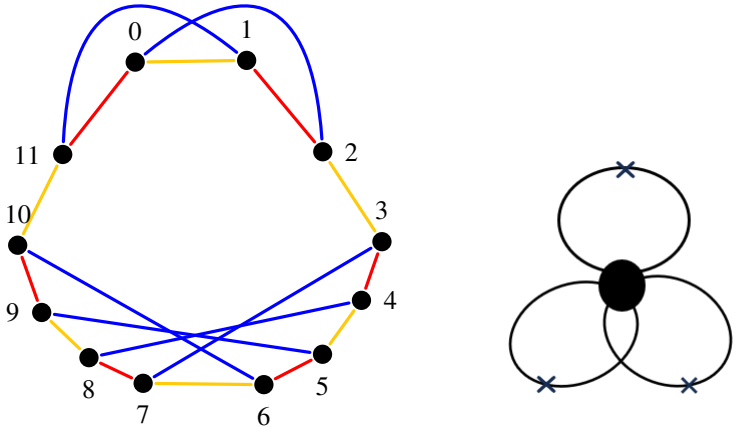

Figure 16: A gem and its corresponding graph showing that the converse of Corollary 8.2 is false.

Single-vertex embeddings are an important special class of embeddings that have been studied from a number of perspectives, and have connections to other ideas such as chord diagrams. A *chord diagram* consists of a circle drawn in the plane, with a finite number of (straight-line) chords with disjoint sets of ends. Since every connected embedded graph has at least one single-vertex partial dual, it is natural, as a strengthening of the result in the previous subsection, to ask which embeddings (a subset of those from Theorem 8.1) have the property that all partial duals are single-vertex. Note that this is equivalent to all partial duals being single-face. In this subsection we answer this question.

Consider an embedded graph $\boldsymbol{G}$ all of whose partial duals are single-vertex. The effects of taking a partial dual with respect to a single edge are detailed in [17, Section 2.2]. If an embedded graph has an untwisted loop, then taking the partial dual with respect to that loop splits the incident vertex into two vertices. So $\boldsymbol{G}$, and all partial duals of $\boldsymbol{G}$, contain no untwisted loops. Clearly, all edges of $\boldsymbol{G}$ are loops, so all edges in $\boldsymbol{G}$ are twisted loops. Two loops e and f are *interlaced* if they share a common vertex v and the cyclic order of edge labels around v is of the form $e \ldots f \ldots e \ldots f \ldots$. If two twisted loops are interlaced, then taking the partial dual with respect to one of the two twisted loops results in the other loop becoming untwisted. So $\boldsymbol{G}$ has no interlaced twisted loops. If there are no interlaced twisted loops, then taking the partial dual with respect to a noninterlaced twisted loop keeps that edge and all other edges as noninterlaced twisted loops. So we arrive at the following characterization.

Theorem 8.4. *The partial duals of an embedded graph $\boldsymbol{G}$ are all single-vertex (or, equivalently, all single-face) if and only if $\boldsymbol{G}$ has a single vertex, every edge of $\boldsymbol{G}$ is a twisted loop, and no two edges are interlaced.*

A graph is *outerplanar* if it has an embedding in the plane with every vertex on the boundary of the outer face. The end graph of a graph embedding $\boldsymbol{G}$ was defined in Subsubsection 4.2.3; it is 3-regular, and at each vertex two of the edges correspond to edges of color a in the gem $\mathbf{J}$, while the other edges correspond to edges of color f in $\mathbf{J}$. The 'colored end graph', which we will denote by $\mathbf{N}$, transfers these colors to the edges of the end graph.

When $\boldsymbol{G}$ is a single-vertex embedding, $\mathbf{N}$ represents the chord diagram associated with $\boldsymbol{G}$: the edges of color a in $\mathbf{N}$ form a cycle corresponding to the circle of the chord diagram, and the edges of color f in $\mathbf{N}$ form a matching whose elements correspond to the chords. The fact that the edges of $\boldsymbol{G}$ are not interlaced means that the chords of the chord diagram are nonintersecting. Since a chord diagram without intersecting chords can be thought of as a 2-connected 3-regular outerplanar graph, with the circle of the chord diagram forming the boundary of the outer face, we obtain the following.

Having all partial duals single-vertex is a property preserved by (full) duality, which swaps the end graph

with the 3-regular side graph described in Subsubsection 4.2.2. We can define a 'colored side graph', where every vertex is incident with two edges colored a, and one edge colored v. Duality also swaps loops with *coloops*, edges that have the same face on both sides. A coloop is *twisted* if the face traverses the edge twice in the same direction, and *untwisted* if it traverses the edge once in each direction. Duality swaps twisted loops and twisted coloops.

Putting all of this together, we have the following.

Theorem 8.5. *Let **G** be an embedded graph. Then the following are equivalent.*

(a) *The partial duals of **G** are all single-vertex.*

(b) *The partial duals of **G** are all single-face.*

(c) *Every edge of **G** is a twisted loop and the colored end graph of **G** can be drawn as an outerplanar graph where all outside edges are colored* a.

(d) *Every edge of **G** is a twisted coloop and the colored side graph of **G** can be drawn as an outerplanar graph where all outside edges are colored* a.

We can also state similar theorems about when all partial Petrial duals are single-face and single-zigzag, and when all partial Wilson duals are single-vertex and single-zigzag. We leave the details to the reader.

9 Conclusion

There are two obvious directions in which it would make sense to try to extend the results in this paper.

The first is for delta-matroids. These were introduced by Bouchet, who showed that every embedded graph has an associated delta-matroid [4, 5]. Properties of the delta-matroids associated with embedded graphs have been extensively investigated by Chun, Moffatt, Noble, and Rueckriemen [11, 12]. The twisted duality framework for graph embeddings corresponds to natural operations in their delta-matroids, and these operations can be extended to larger classes of delta-matroids, such as binary delta-matroids. The largest class of delta-matroids for which these operations make sense is the class of *vf-safe* delta-matroids, defined by Brijder and Hoogeboom [6]. It is natural to try to extend our Fano framework to binary delta-matroids, or even to vf-safe delta matroids. A step in this direction has already been taken by Yan and Jin [41, Theorem 3.6], who showed that Theorem 3.6 can be extended to binary delta-matroids. The overall difficulty with this direction of research is that it is unclear what the counterpart of the medial graph is for delta-matroids.

Another possible direction in which our results might be extended is to hypermaps, which are embeddings of hypergraphs in surfaces. There is a representation of hypermaps as edge-colored cubic graphs which generalizes the idea of gems; see [9]. However, there is no obvious counterpart of jewels in this setting, which means that we may perhaps only be able to extend results that can be expressed in terms of gems.

References

[1] J. A. Bondy, U. S. R. Murty, Graph Theory, Springer, London, 2008.

[2] C. Paul Bonnington, Marston Conder, Margaret Morton, Patricia McKenna, Embedding digraphs on orientable surfaces, J. Combin. Theory Ser. B 85(1) (2002), 1–20.

[3] C. Paul Bonnington, Charles H. C. Little, The foundations of topological graph theory, Springer-Verlag, New York, 1995.

[4] André Bouchet, Greedy algorithm and symmetric matroids, Math. Programming 38(2) (1987), 147–159.

[5] André Bouchet, Maps and Δ-matroids, Discrete Math. 78(1-2) (1989), 59–71.

[6] Robert Brijder, Hendrik Jan Hoogeboom, Nullity and loop complementation for delta-matroids, SIAM J. Discrete Math. 27(1) (2013), 492–506.

[7] S. Chmutov, Generalized duality for graphs on surfaces and the signed Bollobás-Riordan polynomial, J. Combin. Theory Ser. B 99 (2009), 617–638.

[8] Antonio Breda d'Azevedo, Domenico A. Catalano, Jozef Širáň, Bi-rotary maps of negative prime characteristic, Ann. Comb. 23 (2019) 27–50.

[9] S. Chmutov, F. Vignes-Tourneret, Partial duality of hypermaps, Arnold Math. J. 8(3-4) (2022), 445–468.

[10] H. S. M. Coxeter, The densities of the regular polytopes, Math. Proc. Camb. Phil. Soc. 27(2) (1931), 201–211.

[11] Carolyn Chun, Iain Moffatt, Steven D. Noble, Ralf Rueckriemen, Matroids, delta-matroids and embedded graphs, J. Combin. Theory Ser. A 167 (2019), 7–59.

[12] Carolyn Chun, Iain Moffatt, Steven D. Noble, Ralf Rueckriemen, On the interplay between embedded graphs and delta-matroids, Proc. Lond. Math. Soc. (3) 118(3) (2019), 675–700.

[13] Q. Deng, X. Jin, M. Metsidik, Characterizations of bipartite and Eulerian partial duals of ribbon graphs, Discrete Math 343 (2020), Paper 111637.

[14] Blake Dunshee, Directedness, Duality, and Parity Conditions for Embedded Graphs, PhD dissertation, Vanderbilt University, 2020.

[15] M. N. Ellingham, Xiaoya Zha, Partial duality and closed 2-cell embeddings, J. Comb. 8(2) (2017), 227–254.

[16] J. A. Ellis-Monaghan, I. Moffatt, Twisted duality for embedded graphs, Trans. Amer. Math. Soc. 364 (2012), 1529–1569.

[17] J. A. Ellis-Monaghan, I. Moffatt, Graphs on Surfaces: Dualities, Polynomials, and Knots, Springer Briefs in Mathematics, Springer, New York (2013).

[18] Massimo Ferri, Una rappresentazione delle n-varietà topologiche triangolabili mediante grafi $(n+1)$-colorati, Boll. Un. Mat. Ital. B (5) 13(1) (1976), 250–260.

[19] Massimo Ferri, Carlo Gagliardi, Alcune proprietà caratteristiche delle triangolazioni contratte, Atti Sem. Mat. Fis. Univ. Modena 24(2) (1975), 195–220.

[20] M. Ferri, C. Gagliardi, L. Grasselli, A graph-theoretical representation of PL-manifolds – a survey on crystallizations, Aequationes Math. 31(2-3) (1986), 121–141.

[21] J. L. Gross, T. W. Tucker, Topological Graph Theory. Dover Publications, Mineola, NY, 2001.

[22] R.-X. Hao, A note on the directed genus of $K_{n,n,n}$ and K_n. Ars Math. Contemp. 14(2) (2018), 375–385.

[23] S. Huggett, I. Moffatt, Bipartite partial duals and circuits in medial graphs, Combinatorica 33 (2013), 231–252.

[24] Johannes Kepler, Harmonices Mundi Libri V (Five Books of the Harmony of the World), Johannes Plank for Gottfried Tampach, Linz, Austria (1619).

[25] S. Lins, Graphs of Maps, Ph.D. dissertation, University of Waterloo, Canada, 1980; available as `arXiv:math/0305058`.

[26] S. Lins, Graph-encoded maps, J. Combin. Theory Ser. B 32 (1982), 171–181.

[27] C. H. C. Little, A. Vince, Embedding schemes and the Jordan curve theorem, in Topics in combinatorics and graph theory (Oberwolfach, 1990), Physica, Heidelberg, 1990, pp. 479–489.

[28] Metrose Metsidik, Eulerian and even-face partial duals, Symmetry 13(8) (2021), Paper 1475.

[29] Metrose Metsidik, Xian'an Jin, Eulerian partial duals of plane graphs, J. Graph Theory 87(4) (2018), 509–515.

[30] Bojan Mohar, Carsten Thomassen, Graphs on surfaces, Johns Hopkins University Press, Baltimore, MD, 2001.

[31] A. Nakamoto, Y. Suzuki, Partially broken orientations of Eulerian graphs on closed surfaces, Discrete Math. 347(7) (2024), Paper 114016, 8 pp.

[32] Mario Pezzana, Sulla struttura topologica delle varietà compatte, Atti Sem. Mat. Fis. Univ. Modena 23(1) (1974), 269–277.

[33] Neil Robertson, Pentagon-generated trivalent graphs with girth 5, Canadian J. Math. 23 (1971), 36–47.

[34] Saul Stahl, Generalized embedding schemes, J. Graph Theory 2(1) (1978), 41–52.

[35] W. T. Tutte, On the imbedding of linear graphs in surfaces, Proc. London Math. Soc. (2) 51 (1949), 474–483.

[36] Andrew Vince, Combinatorial maps, J. Combin. Theory Ser. B 34(1) (1983), 1–21.

[37] Douglas B. West, Introduction to graph theory, Prentice Hall, Upper Saddle River, NJ, 1996.

[38] Stephen E. Wilson, Riemann surfaces over regular maps, Canad. J. Math. 30(4) (1978), 763–782.

[39] S. E. Wilson, Operators over regular maps, Pacific J. Math. 81(2) (1979), 559–568.

[40] Qi Yan, Xian'an Jin, Extremal embedded graphs, Ars Math. Contemp. 17(2) (2019), 637–652.

[41] Qi Yan, Xian'an Jin, Eulerian and bipartite binary delta-matroids, Acta Math. Appl. Sin. Engl. Ser. 38(4) (2022), 813–821.